

UCSF

UC San Francisco Electronic Theses and Dissertations

Title

Understanding the cellular pathogenesis of Huntington's disease

Permalink

<https://escholarship.org/uc/item/5r13p3jw>

Author

Mitra, Siddhartha

Publication Date

2007-08-30

Peer reviewed|Thesis/dissertation

Understanding the cellular pathogenesis of Huntington's Disease

by

Siddhartha Mitra

DISSERTATION

Submitted in partial satisfaction of the requirements for the degree of

DOCTOR OF PHILOSOPHY

in

Biomedical Sciences

in the

GRADUATE DIVISION

of the

UNIVERSITY OF CALIFORNIA, SAN FRANCISCO

Acknowledgements

I would like to thank my advisor, Steve Finkbeiner for his creative insight, encyclopedic knowledge, and vast reserves of patience. It is a true gift to work with someone like Steve who loves what he does and spreads his enthusiasm widely. The best times in my graduate school years have been talking science with Steve. Thanks also go to my committee members, Robert Edwards and Robert Messing. I have appreciated all their feedback and the warmth with which they have imparted their advice. Thanks should also go to Vishwanath Lingappa with whom I had a great start to my UCSF career.

I would like to thank all the members of the Finkbeiner lab. The supportive environment and collegial atmosphere made going to work pleasant. In particular, I'd like to thank John Bradley and Montserrat Arrasate for all the laughs and a bit of good science as well.

I have progressed to where I am only because of my parents and my accomplishments are theirs more than mine. I can only hope to do the same for my loved ones.

I would also like to thank my wife, Sarah Minick, though there is not enough time or space to thank her properly. Perhaps the most appropriate thing I can do here is to thank her for her help in the preparation of this document, as without her, it would not have been completed.

Understanding the cellular pathogenesis of Huntington's disease

by

Siddhartha Mitra

Abstract

Huntington's disease is a devastating inherited neurodegenerative disorder without a cure. Mutations expanding a stretch of glutamines in the first exon of the widely-expressed huntingtin protein are responsible for Huntington's disease. The disease is characterized by neuronal death within the striatum and cortex. At the cellular level, abnormal inclusions of ubiquitinated huntingtin are present in affected brain areas. The role of inclusions in cellular pathogenesis has been controversial, with inclusions potentially playing protective, detrimental, or incidental roles. We developed a high-throughput robotic imaging and analysis platform that enables us to follow the fates of individual cells and intracellular proteins over time. This platform represents a significant improvement over standard approaches of cell-population based biochemistry and conventional time-lapse microscopy in being able to monitor molecular changes as they unfold in large numbers of live cells and in quantifying the extent to which these changes predict cellular outcomes. Using this platform, we followed individual neurons expressing mutant huntingtin and determined that cells that form inclusions survive better than those that do not. Levels of mutant protein were higher in those cells that formed inclusions and in those cells that died earlier. Through the use of fluorescent reporters of ubiquitin-proteasome system function, we determined that impairment of the ubiquitin-proteasome system is toxic to neurons and is higher in cells that go on to form inclusions compared to those that do not. Following inclusion formation, ubiquitin-proteasome system function is improved. Our data unambiguously shows that inclusions are beneficial to neuronal survival and that part of this beneficial effect may be through improving ubiquitin-proteasome system function. These findings shift the focus to steps preceding inclusion formation in the search for the molecular species responsible for Huntington's disease.

Table of Contents

List of Figures	viii
Chapter 1: An introduction to Huntington's disease	1
Neurodegenerative disease and the aging population	1
Signs and symptoms of Huntington's disease	3
HD belongs to a family of diseases caused by an expansion in CAG repeats	4
CAG repeats are unstable	5
Polyglutamine expansion predicts age of onset	5
Selective neuronal death	6
Gain of toxic function	6
Proteolysis and nuclear localization	7
Inclusion bodies are a hallmark of Huntington's disease	8
Chaperones	8
The ubiquitin-proteasome system	9
Autophagy	10
Autophagy and the UPS	11
Aims and findings of the dissertation	12
Chapter 2: Applying a novel acquisition and analysis platform to understand the cellular pathogenesis of Huntington's disease	13
Abstract	13
Introduction	13
Results	16
A new system for studying cellular pathogenesis	16
Following physiology using fluorescent proteins	17
Htt toxicity is dependent on polyQ expansion	19
PolyQ length and intracellular dosage predict IB formation	20
IBs are protective	22
Diffuse mutant protein is toxic	23
Discussion	25

Materials and Methods	26
Plasmids	26
Cell culture	26
Transfection	27
Live-cell imaging and analysis	28
Chapter 3: Understanding the role of the ubiquitin-proteasome system in the pathogenesis of Huntington’s disease	30
Abstract	30
Introduction	31
Results	33
Single-cell longitudinal analysis of ubiquitin-proteasome function in primary neurons	33
UPS reporters do not respond to inhibition of macroautophagy	37
Proteasome inhibition is not sufficient to induce macroautophagy in primary neurons	37
Neuronal toxicity is proportional to the extent of proteasome inhibition	39
Dynamic changes in UPS function in a primary striatal model of HD	41
Proteasome impairment precedes IB formation	42
Proteasome impairment decreases following IB formation	44
Neurons that form IBs survive better than those that do not	45
Discussion	46
Materials and Methods	48
Plasmids	48
Cell culture	49
Transfection and pharmacology	50
Live-cell imaging and analysis	51
Chapter 4: Concluding remarks	52
Understanding cause-effect relationships underlying disease	52
The particular challenge of the nervous system	52
A new approach	53
Summary of findings	53

Parallels in other neurodegenerative diseases	54
The toxic species	55
Mechanisms of toxicity	56
The need for therapies	56
References	58
Appendix 1:	
<i>Trans</i>-acting factors and the cellular pathogenesis of HD	74
Chaperones	75
Ubiquitin-proteasome system	79
Autophagy	82
Interacting proteins	83

List of Figures

- Figure 1.1. Rapid growth in older demographics. •1
- Figure 2.1. Primary neurons expressing GFP or RFP have comparable survival. •17
- Figure 2.2. The presence of serum in the media after transfection has no effect on primary neuronal survival. •17
- Figure 2.3. Monitoring a httQ72 expressing cell that forms an IB. •18
- Figure 2.4. Htt toxicity is proportional to polyQ length in primary neurons. •19
- Figure 2.5. Htt toxicity is proportional to polyQ length in PC12 cells. •20
- Figure 2.6. Htt toxicity is proportional to polyQ length in PC12 cells stably expressing an inducible htt transgene. •20
- Figure 2.7. IBs form earlier as the polyQ expansion increases. •21
- Figure 2.8. Cells that form IBs survive longer than those without. •22
- Figure 2.9. IB formation is not required for polyQ dependent toxicity in neurons. •23
- Figure 2.10. IB formation is not required for polyQ dependent toxicity in PC12 cells. •23
- Figure 2.11. Intracellular htt level predicts the duration of cell survival. •24
- Figure 3.1. Levels of GFP^u increase following MG132 treatment. •34
- Figure 3.2. Levels of mRFP^u increase following MG132 treatment. •35
- Figure 3.3. Levels of Venus^u and Ub^{G76V}-Venus increase following epoxomicin treatment. •36
- Figure 3.4. Limited interaction between the UPS and autophagic pathways in neurons. •38
- Figure 3.5. UPS reporter fluorescence shows a dose dependent response to MG132 treatment. •39
- Figure 3.6. UPS reporter fluorescence continues to increase up to 12 hours after the addition of MG132. •39
- Figure 3.7. MG132 is toxic to neurons in a dose-dependent fashion. •40
- Figure 3.8. Three color longitudinal imaging of primary neurons in culture. •42
- Figure 3.9. UPS impairment precedes IB formation at 54 hours after transfection. •43
- Figure 3.10. UPS impairment precedes IB formation at 76 hours after transfection. •43
- Figure 3.11. An improvement in UPS function follows IB formation. •44

Figure 3.12. Neurons that form IBs at 18 hours post-transfection

survive longer than those that do not form IBs. •45

Figure 3.13. Neurons that form IBs at 27 hours post-transfection

survive longer than those that do not form IBs. •45

Figure 4.1. Ataxin-1 demonstrates polyQ-independent toxicity in primary cortical neurons. •54

Figure 4.2. Mutants of SOD1 that cause ALS are toxic to primary striatal neurons. •55

Figure A.1. Hsp70 either increases survival or htt levels in cells with mutant htt. •76

Figure A.2. Hsp40 or DNAJA2 have no consistent effect on survival in cells with mutant htt. •77

Figure A.3. Hsp104 generally increases the toxicity of mutant htt. •78

Figure A.4. REGg and REGg(K->E) increase the toxicity of mutant htt. •79

Figure A.5. cdc34DN has no consistent effect on mutant htt toxicity. •80

Figure A.6. Wild-type or chain terminating ubiquitin potentiate mutant htt toxicity. •81

Figure A.7. HDAC6 has no effect on mutant htt toxicity but increases mutant htt IB formation. •82

Figure A.8. mTOR has no effect on mutant htt toxicity or IB formation. •82

Figure A.9. HIPPI decreases mutant htt toxicity but has no effect on IB formation or htt levels. •83

Chapter 1: An introduction to Huntington's disease

Neurodegenerative disease and the aging population

In the next 50 years, the number of elderly in the United States population is projected to skyrocket. The US Census Bureau projects that the total US population will grow almost fifty percent by the year 2050 with the most dramatic growth in the number of people 65 and over. The 65-84 demographic will more than double and the population over 85 years of age will grow to almost five times its current size (Fig 1.1). As the proportion of older citizens increases (Fig 1.1), diseases that are age dependent will increase in prevalence.

Neurodegenerative disease is already the sixth leading killer in the United States (Table 1). The majority of this burden is from Alzheimer's disease, which itself is the seventh leading cause of death and is estimated to cost the United States between 30 and 90 billion dollars a year.¹ Moderate estimates indicate that between eight and thirteen million people will be suffering from Alzheimer's disease by the year 2050,² four times as many people as are currently affected.

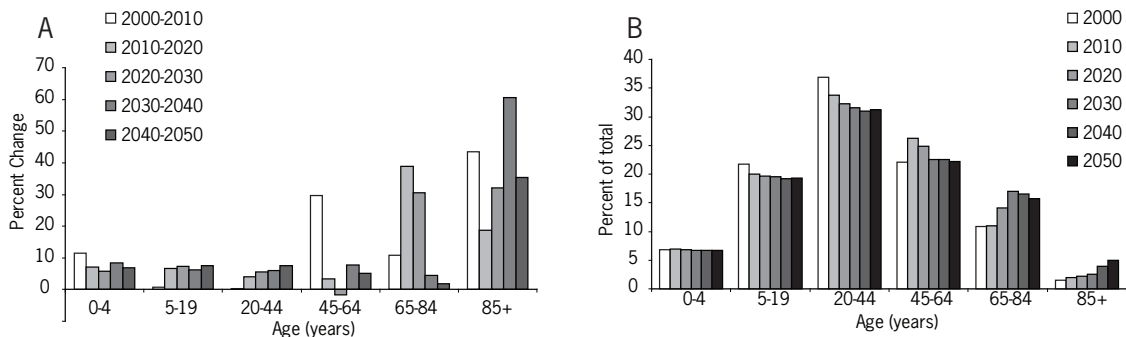


Figure 1.1. Rapid growth in older demographics. (A) US Census Bureau projections showing population growth in the US, stratified by age group. Though the US population is expected to grow by 50 percent by the year 2050, the 65-84 year old demographic will grow by over 110 percent and population older than 84 will grow by over 350 percent. (B) US Census bureau projections by decade for the proportion of the total US population in a particular age group. The proportion of older people (65-84+) in the US will grow over the next 40 years while the proportion of younger people (0-44) will shrink.

Rank	Cause of Death (based on the International Classification of Diseases, Tenth Revision, 1992)	Number
	All causes	2,398,365
1	Diseases of heart	654,092
2	Malignant neoplasms	550,270
3	Cerebrovascular diseases	150,147
4	Chronic lower respiratory diseases	123,884
5	Accidents (unintentional injuries)	108,694
6	Diabetes mellitus	72,815
7	Alzheimer's disease	65,829
8	Influenza and pneumonia	61,472
9	Nephritis, nephrotic syndrome and nephrosis	42,762
10	Septicemia	33,464
11	Intentional self-harm (suicide)	31,647
12	Chronic liver disease and cirrhosis	26,549
13	Essential (primary) hypertension and hypertensive renal disease	22,953
14	Parkinson's disease	18,018
15	Pneumonitis due to solids and liquids	16,959
	All other causes	418,810

Table 1.1. Leading causes of mortality in the US. National Center for Health Care Statistics estimates of causes of mortality from 2004. Out of roughly 2.4 million deaths in the US in 2004, the two most common neurodegenerative diseases, Alzheimer's disease and Parkinson's disease, account for a total of 84,000 deaths.

Though Parkinson's disease, amyotrophic lateral sclerosis, and Huntington's disease affect fewer people than Alzheimer's disease, intriguing commonalities between these neurodegenerative diseases offer the hope that by understanding any one, we may be able to better address the others. Each neurodegenerative disease increases in incidence with age, affects the nervous system, and inexorably leads to death, but only Huntington's disease is predominantly inherited, with an identified initiating cause for the majority of disease. As in the case of other neurodegenerative diseases, there is no cure for Huntington's disease or any treatment that slows progression. The lack of a cure combined with an identified genetic cause makes Huntington's disease a compelling disorder to study. By investigating Huntington's disease, we will also better understand neuronal homeostasis and cellular physiology.

Signs and symptoms of Huntington's disease

Huntington's disease (HD) is estimated to affect five to seven in 100,000 people, though up to ten-fold fewer are affected in Asian and African populations.³ HD most often presents in the fourth or fifth decade of life, though the onset of disease has been documented from ages of 1 through 80 years.^{4,5} Changes in personality, motor control and cognition have been described. Prior to diagnosis, many HD patients exhibit symptoms as well, though these are less consistent and the patient may not be cognizant of them at the time.³

Preceding clinical diagnosis, behavioral changes are prevalent. Individuals often become irritable or disinhibited and changes in mood are common. Individuals at risk for HD often show signs of depression with increases in suicidal ideation.⁶ Patients are less adept at recognizing negative emotions in others, such as anger, disgust, fear, and sadness, both preceding and following diagnosis.⁷⁻⁹ Family members often detect signs of restlessness or fidgeting that are difficult for the patient to recognize.

In early stages, cognitive changes are also common. Pre-symptomatic HD is marked by impairments in memory formation and retrieval and patients often have impaired verbal episodic memory.¹⁰ When movement abnormalities first develop, the patient may only recognize the effects and not the causes of the motor impairment; patients often complain of clumsiness, dropping objects, or falling.¹¹

As the disease progresses, HD is accompanied by more specific symptoms. Patients may be diagnosed with HD from primarily motor, psychiatric, or cognitive disabilities. At the time of clinical diagnosis, most patients demonstrate chorea or dystonia and rigidity, a lack of coordination, motor impermanence and saccadic eye movements.³ Though chorea is one of the most frequent symptoms and most emblematic of the disease, it is a poor indicator of disease severity or progression. Juvenile patients affected by HD often present with dystonia rather than chorea and in older patients, progression is often

accompanied by a decrease in chorea and an increase in dystonia and rigidity.¹² The age of disease onset appears to relate to the rate of disease progression, with earlier ages relating to faster progression, though there has been a considerable amount of controversy about this relationship. Older studies demonstrate no relationship,¹²⁻¹⁴ but newer methodology finds an association between onset and progression^{4,5} though it may be the strongest for juvenile onset HD.¹⁵

HD belongs to a family of diseases caused by an expansion in CAG repeats

A major breakthrough in understanding the pathogenesis of HD occurred when the gene responsible for the disease was cloned. Though chromosome 4 had been implicated in HD from linkage disequilibrium studies in 1983,¹⁶ the gene responsible for HD was identified ten years later on the short arm of chromosome 4 at the 4p16.3 locus.¹⁷ Alternately denominated *IT15*, *HD*, and *HTT*, the gene codes for a widely expressed 348 kDa protein with a polymorphic CAG trinucleotide repeat.

At the time, genes for only three other trinucleotide repeat disorders had been identified, only one of which was present in the coding sequence of the gene. A CGG repeat in the 5' untranslated region of the *FMRI* gene had been identified as the cause of Fragile-X Mental Retardation¹⁸⁻²⁰ and a CTG repeat in the 3' untranslated region of the *MtPK* gene had been identified as the cause of a dominant form of myotonic dystrophy.²¹ ²² The gene responsible for X-linked spinobulbar muscular atrophy (SBMA) had also been cloned; an unstable CAG repeat in the coding region of the androgen receptor (AR) is responsible for the disease.²³

There are now seven other neurodegenerative diseases that have been identified to be caused by an increase in CAG repeat length. With the exception of SBMA, which is X-linked recessive, all are autosomal dominant in inheritance. Spinocerebellar ataxias (SCA) 1, 2, 3, 6, 7, and 17 are caused by CAG repeat expansions in the ataxin 1, 2, 3,

6, 7, and TBP genes and affect primarily the cerebellum and brainstem. Dentatorubral pallidoluysian atrophy (DRPLA) is caused by a CAG repeat expansion in the atrophin 1 gene and also affects the cerebellum as well as the cortex and midbrain.²⁴

The effect of CAG repeat expansion is dependent on the gene context of the repeat. Brain regions first affected by each disease vary as does the threshold number of repeats needed to cause disease. While CAG repeat expansion past 36-39 triggers HD, SBMA, SCA 1, 2, and 7, longer repeats are necessary for SCA 3 and DRPLA,^{25, 26} and shorter repeats are sufficient for SCA 6.²⁷

CAG repeats are unstable

From genetic analysis of patients affected by the disease, CAG repeat length has been seen to vary in individual cells of patients and through transmission from parent to child. The instability in the number of CAG repeats in *HD* has been of great interest since preventing expansion would decrease the impact of the disease in the future and potentially in currently affected individuals as well. Anticipation is a common feature in the inheritance of trinucleotide repeat disorders in which the trinucleotide repeat number increases upon transmission from parent to child.²⁸ In the case of HD, the number of CAG repeats increases most dramatically in paternal transmission^{28, 29} and is likely a result of DNA replication during spermatogenesis.^{30, 31} An increase in CAG repeat number occurs in somatic cells as well, especially in the brain.³² New evidence indicates that a combination of oxidative DNA damage and error-prone repair may explain a significant amount of trinucleotide repeat expansion.^{33, 34}

Polyglutamine expansion predicts age of onset

The CAG repeats underlying HD translate into a homomeric polyglutamine (polyQ) stretch in the amino-terminus of the huntingtin (htt) protein. Not only does

the expansion of the polyQ stretch above a threshold of 36 glutamines in the htt protein (mutant htt) initiate disease, but the length of the stretch is inversely proportional to the age of HD onset. PolyQ length may explain more than seventy percent of the variation in the age of disease onset^{28, 29, 35, 36} and can be used in a parametric model to accurately predict disease incidence.³⁷

Selective neuronal death

As the disease progresses, mutant htt leads to the death of specific neuronal subpopulations. Medium spiny neurons in the striatum expressing enkephalin and γ -amino butyric acid are particularly susceptible to mutant htt.³⁸ The medial paraventricular region and tail of the caudate along with the dorsal putamen are the first brain regions to show significant atrophy.³⁹ Neuronal death that begins in the striatum spreads and with time, there is significant volume loss in the cortex, white matter, and thalamus.^{40, 41} Though both normal and mutant htt are widely expressed in the brain and other tissues,^{42, 43} brain regions and cell types vary in levels of htt expression and this variation may explain some of the specificity of cell death seen in HD brain.⁴⁴

Gain of toxic function

The central question in understanding HD is why mutant htt triggers dysfunction and cell death. The genetics of HD and other CAG repeat disorders strongly support the hypothesis that polyQ expansion leads to a toxic activity that is not present for shorter polyQ stretches. HD is inherited in an autosomal dominant pattern with almost complete penetrance when the gene contains more than 40 CAG repeats.³⁷

In mice, the loss of *Hdh*, the mouse *HTT* homolog, results in embryonic lethality,⁴⁵ supporting the possibility that the normal function of htt is required during brain development, but is largely unrelated to the HD phenotype.⁴⁷ Mutant htt is sufficient

to rescue the embryonic lethal phenotype, arguing that mutant htt retains significant activity.⁴⁸ Though brain and testis specific inactivation of *Hdh* results in age-related neurodegeneration, the mice do not resemble HD models in pathology or phenotype.⁴⁹

Proteolysis and nuclear localization

Accompanying the gain of toxic function, full length mutant htt is cleaved into amino-terminal fragments. An amino-terminal fragment of mutant htt is sufficient to cause a large number of detrimental effects in the brain, including inhibiting glutamate reuptake and release,^{50, 51} blocking axonal transport,^{52, 53} sequestering transcription factors,⁵⁴ altering electrophysiology,^{55, 56} and increasing susceptibility to excitotoxic injury.^{57, 58} Furthermore, an exon 1 fragment of mutant htt is sufficient to cause a progressive neurodegenerative phenotype resembling HD in mice.⁵⁹

The cleavage event generating the fragments likely occurs in the cytoplasm after which fragments move into the nucleus and frequently aggregate. This phenomenon is seen most frequently in striatal neurons in mouse models of disease and may partly account for the susceptibility of the striatum to disease.^{50, 60}

There has been a considerable amount of research to determine which protease is responsible for generating these fragments, but its identity is still unclear. Early evidence pointed to a cysteine protease⁶¹ and caspase 3 seemed a likely candidate.⁶²⁻⁶⁴ However, many of these findings were complicated by the general pro-survival effect of caspase inhibition.⁶⁵⁻⁶⁷ One study identifies aspartyl protease activity that generates two N-terminal fragments of mutant htt that are usually rapidly degraded.⁶⁸ More recently, a caspase 6 site in htt has been identified to be required for htt-mediated striatal neurodegeneration, but may regulate neuronal response to injury generally.⁶⁹

Inclusion bodies are a hallmark of Huntington's disease

No matter what the culprit, the generation and deposition of amino-terminal mutant htt fragments in large, microscopically visible inclusion bodies (IBs) is a hallmark of HD.^{70,71} Mutant htt expression is sufficient for IB formation in HD. Though IBs may vary in composition,⁷² they are present in the same populations of neurons in humans and mice that undergo death and dysfunction in the course of disease.^{50,70,71}

IBs are present in the nucleus, cytoplasm, and processes of neurons and contain both mutant htt and other proteins. Though mutant htt initiates IB formation, wild-type htt is also recruited into these structures and sequestration of wild-type htt may contribute to the progression of HD.⁷³ Mutant htt IBs either colocalize with or contain transcriptional repressors^{74,75} and activators,⁷⁶⁻⁷⁸ likely perturbing transcription by changing the distribution of transcriptional machinery.⁷⁹⁻⁸² IBs also contain many components of intracellular machinery responsible for handling and degrading misfolded protein, including chaperones, ubiquitin, proteasome subunits, and autophagic machinery.^{70,71,78,83}

The presence of the intracellular quality control machinery for misfolded protein in IBs suggests IB formation may be due to the inability of mutant htt protein to fold or be degraded.

Chaperones

Many chaperones assist with co-translational and post-translational folding of proteins. There are numerous heat shock proteins (Hsps), some of which are constitutively expressed and some of which are induced after cell stress. One major family of Hsps containing both constitutive and induced members is the Hsp70 family. Hsp70s are evolutionarily well-conserved and are present in all compartments of the cell. They bind to linear stretches of hydrophobic amino acids in polypeptides and their binding to substrates is regulated by ATP hydrolysis. Hsp40s, including Hdj1, assist in activating

Hsp70s for substrate binding, though some Hsp40 family members such as Hdj2 may have intrinsic refolding activity themselves. Hsp90 family members also stabilize misfolded proteins and accept substrates from Hsp70; this interaction is particularly important in signal transduction by steroid hormone receptors and tyrosine kinases. A number of accessory factors such as Hip, Hop, and Bag-1 modulate the Hsp70 ATP hydrolysis cycle and regulate Hsp-Hsp and Hsp-substrate interactions.⁸⁴

The presence of Hsp40 and Hsp70 in mutant htt IBs⁷⁸ has led to a number of studies in numerous model systems investigating the effect of Hsp40 and Hsp70 in models of polyQ disease. Increasing Hsp40,⁸⁵⁻⁸⁸ Hsp70,^{89,90} or both⁹¹ suppress polyQ IB formation and toxicity in some models, though the effect is sometimes seen only on IB formation or toxicity⁹² and sometimes on neither.⁹³ Interpreting these studies can be difficult since they test models of different polyQ diseases in different organisms or cell culture systems.

The ubiquitin-proteasome system

In the event that protein refolding fails, misfolded proteins are targeted for degradation. One major pathway of intracellular protein degradation is the ubiquitin-proteasome system (UPS). The proteasome is a multicatalytic complex consisting of a 19S regulatory subunit and 20S core that contains chymotrypsin-like, trypsin-like, and post-glutamyl peptidase activities. To target proteins for degradation, ubiquitin, a 76 amino acid polypeptide, forms sequential thioester linkages with cysteine residues on E1 ubiquitin activating enzymes and E2 ubiquitin conjugating enzymes, and with the assistance of E3 ubiquitin ligases, forms an isopeptide bond with the amino group of lysine residues on the substrate.⁹⁴ Several internal lysine residues within ubiquitin can then be used as sites for additional ubiquitin addition. Once a protein is modified by a polyubiquitin chain with a minimum of four ubiquitins, the protein is efficiently targeted to the proteasome for degradation.⁹⁵

Inhibition of the proteasome in proliferating cells causes cell cycle arrest and ensuing cell death. If proteasome inhibition leads to toxicity through an accumulation of toxic proteins, potential mediators include RB, p53, E2F, p21, p27, cyclin D and cyclin E.⁹⁵ This retinue of proteins overlaps significantly with the group of proteins having functions in cell cycle regulation. The relationship between these substrates and the UPS in post-mitotic cells is unclear and the mediators of toxicity from proteasome inhibition are largely unknown.

PolyQ expansion and IB formation have been identified to impair the proteasome.⁹⁶ However, the significance of the relocalization of UPS components to IBs is not clear. Some IBs, such as those formed by ataxin 1 or mutant SOD 1, have fast exchange of protein with the cellular milieu.^{97, 98} Those formed by mutant htt, however, have appeared to be static.⁹⁹ It has yet to be determined if IB formation is beneficial or detrimental to UPS function.

Autophagy

A second major pathway for the turnover of intracellular components is the autophagic pathway. Cytoplasmic components are targeted to the lysosome by three arms of autophagy, microautophagy, chaperone-mediated autophagy and macroautophagy. Macroautophagy has been the best studied and is understood to regulate the availability of precursors for protein and organelle biogenesis. In times of starvation, many cells upregulate macroautophagy to hydrolyze proteins, lipids, nucleic acids, and carbohydrates; induction of macroautophagy is inhibited by mTor and activated by PP2A. After induction, macroautophagy proceeds by the formation of a double membrane structure called the autophagosome, which encloses the cytoplasmic components that will be degraded. Formation of the autophagosome is promoted by class III phosphoinositide 3-kinases (PI3K) and inhibited by class I PI3Ks. The autophagy inhibitor 3-methyladenine

blocks autophagy at this step. This autophagosome is then delivered to the lysosome with which it fuses. The vacuolar ATP-ase inhibitor Bafilomycin A1 blocks fusion of the autophagosome with the lysosome.¹⁰⁰

Atg genes, originally identified in a yeast screen for defective autophagy,¹⁰¹ are responsible for mediating the steps of autophagy. Atg 1, 11, 13, and 17 play a role during induction. Atg 5, 7, 10, 12 and 16 play a role during the formation of the autophagosome.

The autophagic pathway in neurons is less well studied, but shows significant differences from the autophagic pathway in other cell types. Autophagy is not induced in neurons following starvation, likely because it is already active.¹⁰² Mouse knockouts of the essential autophagy genes Atg5 and Atg7 cause an accumulation of ubiquitinated substrates and a neurodegenerative phenotype in mice,^{103, 104} reinforcing the finding that basal autophagy is critical to neuronal survival. Autophagy is important for degrading mutant htt¹⁰⁵ and inhibiting autophagy potentiates mutant htt toxicity.¹⁰⁶

Autophagy and the UPS

Since both UPS and autophagic degradation handle mutant htt, understanding the interaction between the two systems is important for understanding HD pathogenesis. Histone deacetylase 6 (HDAC6) may function as a molecular handle to investigate this link. HDAC6 is important for coupling proteins to IB formation¹⁰⁷ as well as recruiting autophagic machinery to the IB.¹⁰⁸ New research demonstrates that HDAC6 protects against neurodegeneration from mutant protein and impaired UPS function.¹⁰⁹ Examining the effect of HDAC6 on IB formation and neurodegeneration in a mammalian model of HD should yield further insight.

Aims and findings of the dissertation

The relationship between mutant htt, IB formation, intracellular protein degradation, and neurodegeneration has been difficult to address. The difficulty lies in determining if IBs are an intermediary in disease progression or a protective response that prolongs survival. Conventional approaches have yielded contradictory results because they lack the sensitivity and speed to isolate and follow large numbers of cells based on IB formation. Though microscopy techniques have been helpful, they are limited by either low temporal resolution or the ability to gather enough longitudinal data to make relate cellular events and outcomes.

In Chapter 2, we applied a novel platform capable of monitoring single-cells over the course of days to address the question of IBs and toxicity. Prospectively following neurons and PC12 cells expressing mutant htt, we found that cells that form IBs survive better than those that do not. Instead of IB formation, levels of diffuse mutant htt predicted toxicity.

In Chapter 3, we attempted to reconcile the protective effect of IB formation with the observation that mutant htt inhibits the UPS and that cells with IBs show impaired UPS function. We applied a prospective longitudinal approach to follow IB formation, UPS function and toxicity. Our findings included higher UPS impairment preceding IB formation and lower UPS impairment following. These results support a model where IB formation may be protective in part by decreasing the impairment of the UPS.

Chapter 2: Applying a novel acquisition and analysis platform to understand the cellular pathogenesis of Huntington's disease

Abstract

Initiated by the expansion of a stretch of polyglutamines within the huntingtin protein, Huntington's disease results in neuronal death in the striatum and cortex. Within these affected brain regions, neurons develop abnormal inclusion bodies containing accumulations of mutant protein. The role of inclusion bodies has been controversial, with both detrimental and beneficial roles proposed for them. We developed an automated imaging and analysis platform capable of following individual cells over the course of days and applied this system to a primary neuronal model of Huntington's disease. We found that huntingtin is toxic to neurons in a polyglutamine-length dependent manner and that the dose of mutant huntingtin predicts both when inclusion bodies will form and when cells will die. However, cells that form inclusion bodies survive better than those that do not and diffuse mutant huntingtin in the cell is sufficient for polyglutamine-dependent toxicity. Our data supports a model where inclusion body formation is a beneficial coping response to more diffuse forms of toxic mutant protein.

Introduction

Huntington's disease (HD) is a progressive, debilitating neurodegenerative disease inherited in an autosomal dominant manner and characterized by motor abnormalities, behavioral changes and cognitive impairment. No cure exists for HD and treatments to ameliorate symptoms do not halt disease progression.¹¹⁰

Mutations that cause HD result in the expansion of a polymorphic stretch of CAG codons beyond 35 repeats in the huntingtin protein (htt).^{16, 17} CAG repeat expansion translates into the expansion of a homomeric glutamine (polyQ) stretch within the first exon of htt.

The length of the polyQ stretch correlates with an earlier age of disease onset and possibly faster disease progression.^{4,5}

In the course of HD, amino-terminal fragments of mutant htt are deposited in aggregates in the nuclei, cell bodies, and neurites of neurons within the cortex and striatum.⁷⁰ These nuclear inclusion bodies (IBs) stain for ubiquitin and suggest an imbalance between mutant htt production and clearance. Inclusions can form as a result of polyQ expansion in the context of many different proteins in both cell culture models and transgenic mice; as such, inclusion formation by these proteins is mediated at least in part by the polyQ expansion itself.¹¹¹ Most manipulations of yeast, mammalian cell culture, or transgenic mouse models that increase toxicity also increase IB formation and most that decrease toxicity also decrease IB formation. Increases in IB formation and toxicity result from increasing expression of mutant htt protein, heat shock of cells, or by inhibiting chaperone function;¹¹²⁻¹¹⁴ decreases result from decreasing mutant htt expression, overexpressing chaperones, activation of the IGF-1/Akt pathway, or overexpression of parkin, an ubiquitin ligase.¹¹⁵⁻¹¹⁸ These observations led to the hypothesis that IBs lead to neurodegeneration.

This hypothesis is challenged by a number of experiments dissociating IB formation from neuronal toxicity. One series of experiments utilizes mutant ataxin-1, another disease-causing protein containing an expanded polyQ stretch that also forms IBs; however, a self-association domain within mutant ataxin-1 is required for IBs to form. Transgenic mice expressing mutant ataxin-1 with a deleted self-association domain no longer develop IBs but still develop behavioral abnormalities; these behavioral abnormalities are similar to those in transgenic mice expressing mutant ataxin-1 with the self-association domain and IBs.¹¹⁹ A second example of toxicity without IBs is in transgenic mice expressing a yeast artificial chromosome encoding full-length mutant htt with 72 glutamines. Though high levels of transgene expression lead to IBs and

neuropathology, low levels of expression still lead to neuropathology with no IBs present, even when sections are examined by electron microscopy.¹²⁰ A third report questioning a pathogenic role for IBs used primary cultures of striatal neurons transfected with mutant htt. While mutant htt normally forms IBs in these cells, co-transfection of a dominant-negative ubiquitin-conjugating enzyme, *cdc34*, prevents IB formation but increases cell death.¹²¹ These studies demonstrate that IBs are not necessary for toxicity; furthermore, they raise the possibility that IBs may protect cells from neurodegeneration.

Standard approaches of cell population-based biochemistry and conventional time-lapse microscopy have struggled to unravel the relationship between mutant htt, IB formation and neuronal toxicity. The inability to predict which cells will form IBs and when cells will die is compounded by these events occurring asynchronously within individual cells in the same population. Biochemical approaches have been plagued by the inability to distinguish between biologically distinct objects, leading to a limited ability to detect changes and understand cause-effect relationships. Though conventional time-lapse microscopy techniques have been useful to observe successive changes unfold in single cells, they have been limited by labor-intensive and user-biased data acquisition and by an inability to quantitatively monitor and analyze the contribution of cellular changes to particular outcomes.

Using a new experimental platform, we quantitatively and prospectively measured the survival of individual neurons, the intracellular expression of mutant htt, and IB formation in transformed cell lines and in a primary striatal neuron model of HD. We found that mutant htt induced cell death in a polyQ-dependent manner, but that for a given polyQ stretch, toxicity was proportional to the dose of mutant protein. IB formation was associated with improved cellular survival and coincident with a reduction in the levels of toxic mutant htt elsewhere within cells. Our data lead us to conclude that IBs are unlikely to explain the neurodegeneration induced by mutant htt and instead may be part

of a beneficial coping response to toxic mutant protein.

Results

A new system for studying cellular pathogenesis

To quantitatively analyze stochastic processes within single cells with high temporal and spatial resolution, we developed and validated a new experimental platform. The core of the device is an inverted microscope body equipped with computer-controlled motors and special optics for automated collection of images. We developed algorithms to direct the microscope to return to the same fields of cells repeatedly, with the ability to remove the sample from the system between imaging. The instrument automatically focuses itself by using fast Fourier transform analysis of images from different focal planes, collects fluorescent images at different wavelengths, and moves the stage precisely to non-overlapping fields. Even with cells such as primary neurons which have a low (5-20%) transfection efficiency, we can capture images of over 300,000 transfected cells from a single 24-well plate in a low resolution mode or over 6,000 cells with a high resolution mode. These modes allow for the parallel acquisition of independent spectral signals from the same individual cells through the automated placement of spectral filters in the optical path.¹²² The resulting images of multiple signals from individual fields of cells over time are archived for manual or automated analysis. With this platform, we can acquire data with significantly improved speed, sensitivity, and reproducibility over previously employed techniques. By acquiring single-cell data, we can use survival techniques such as Kaplan-Meier curves and Cox proportional hazards analysis to quantify the relative contribution of multiple parameters to outcomes within individual cells.

Following physiology using fluorescent proteins

To visualize intracellular features of live cells over time, we used fluorescent proteins derived from either the jellyfish *Aequorea Victoria*¹²³ or coral of the *Discosoma* genus.¹²⁴ The survival of primary striatal neurons transfected with either enhanced green fluorescent protein (eGFP) or monomeric red fluorescent protein 1 (mRFP) was comparable (Fig 2.1) and independent of the presence of serum following transfection (Fig 2.2).

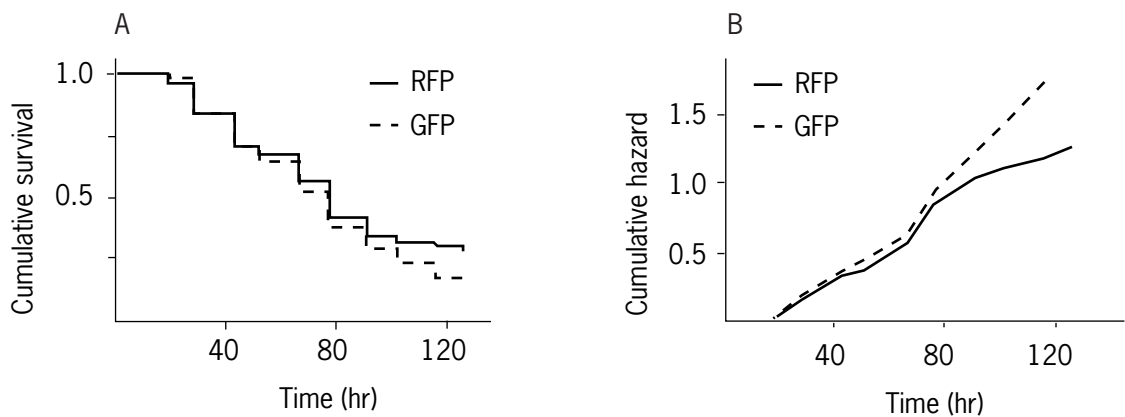


Figure 2.1. Primary neurons expressing GFP or RFP have comparable survival. E17 rat striatal neurons grown 5 DIV were transfected with $1\mu\text{g}$ pGW1-GFP or pGW1-mRFP and followed for 6 days after transfection. Kaplan-Meier curves showing cumulative survival (A) or cumulative hazard (B) are not significantly different. Cumulative hazard is the quantification of the cumulative risk of death of a single object in the treatment condition over the course of the experiment.

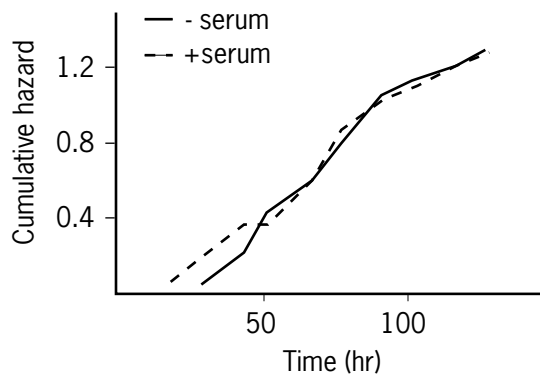


Figure 2.2. The presence of serum in the media after transfection has no effect on primary neuronal survival. E17 striatal neurons were grown 5 DIV, transfected with $1\mu\text{g}$ pGW1-mRFP and followed for 6 days after transfection. Kaplan-Meier cumulative hazard curves are not significantly different.

We then used a previously characterized primary neuronal model of HD¹²¹ to follow the effects of introducing htt into live cells. We transiently transfected plasmids encoding the first exon of the htt protein containing 17, 46, 72, and 97 glutamines (17Q, 46Q, 72Q, 97Q) into rat striatal neurons. To visualize htt, we fused eGFP to the carboxy-terminus of the first exon of htt. We simultaneously introduced mRFP into these cells to monitor the integrity of the plasma membrane.¹²⁵ Following individual transfected cells over time, we simultaneously monitored the intracellular levels of htt protein, the formation of htt IBs, and the survival of transfected neurons (Fig 2.3).

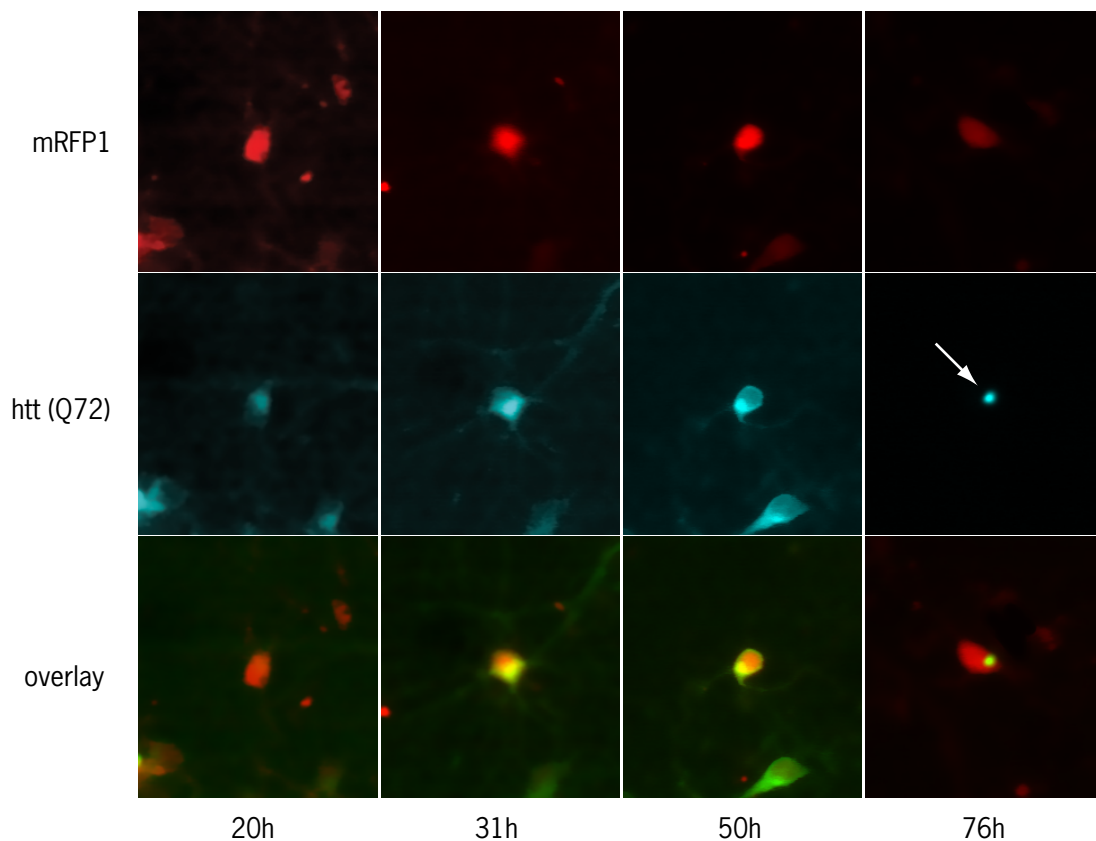


Figure 2.3. Monitoring a httQ72 expressing cell that forms an IB. HttQ72GFP and mRFP in the same field of primary striatal neurons were imaged at the intervals shown. Survival was monitored by the presence of mRFP fluorescence in the cell body (top row). Htt levels and IB formation was followed by GFP fluorescence (middle). The cell in the center of the field is alive at the end of the series, but forms an IB (arrow) between 50 and 76 hours after transfection.

Htt toxicity is dependent on polyQ expansion

In this primary striatal model of HD, we found that the survival of neurons with httQ17 was comparable to that of neurons with eGFP alone. However, neurons transfected with either httQ47, httQ72 or httQ97 die significantly faster than httQ17. The risk of death for neurons containing htt increases as the polyQ tract within htt lengthens (Fig 2.4).

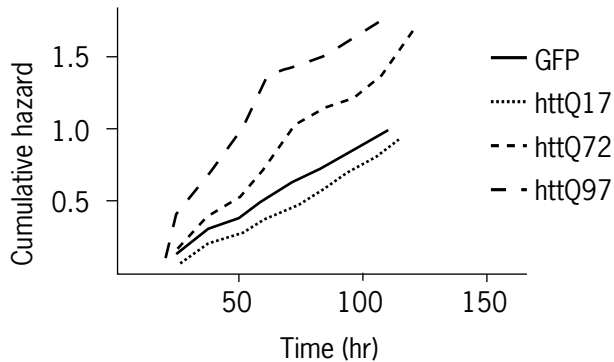


Figure 2.4. Htt toxicity is proportional to polyQ length in primary neurons. E17 primary striatal neurons were transfected 7DIV with GFP, httQ17GFP, httQ72GFP, or httQ97GFP and mRFP. Neurons expressing GFP and httQ17GFP have comparable hazard functions. The risk of death increases in httQ72GFP and is even higher in httQ97GFP. (ns, $p < 0.01$, $p < 0.001$; $n > 200$, 2 experiments)

Since our primary rat striatal cultures are composed of many types of neurons and contain some glia, cell-type-specific effects may confound the association between increased polyQ tract length and toxicity. To exclude this possibility, we examined the effect of introducing htt into a pheochromocytoma cell line (PC12). PC12 cells have many properties of neurons but are clonal, which decreases the contribution of genetic and epigenetic effects to the survival differences between experimental conditions. We transiently transfected htt with varied length polyQ tracts into PC12 cells and followed the survival of these cells. Similar to our results in primary neurons, we found that PC12 cells expressing httQ17 or httQ25 survive significantly better than cells with httQ46, httQ72 or httQ97. Again, as the polyQ tract increases in length above the threshold of 36, toxicity also increases (Fig 2.5). We also examined stably-transfected cells that inducibly express httQ25 or httQ103. After induction, we found that cells expressing httQ25 also survive significantly better than those expressing httQ103 (Fig 2.6).

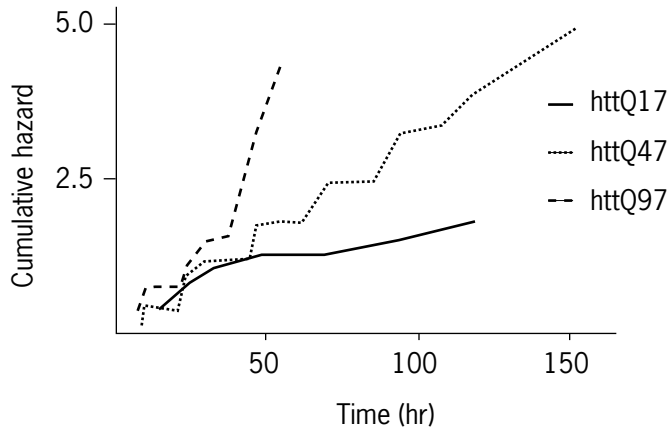


Figure 2.5. Htt toxicity is proportional to polyQ length in PC12 cells. Wild-type PC12 were transiently transfected with httQ17, httQ46 or httQ97 and mRFP. The risk of death is low for httQ17 but increases for httQ46 and continues to increase for httQ97 ($p < 0.001$, $p < 0.001$; $n > 200$, 2 replicates).

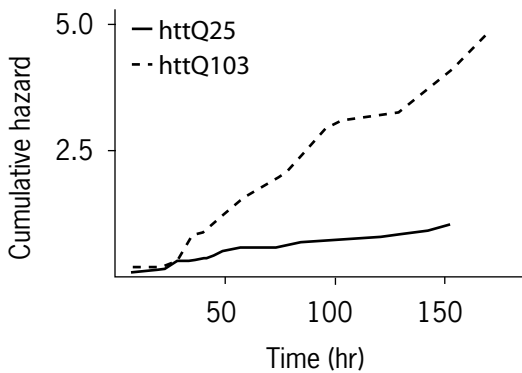


Figure 2.6. Htt toxicity is proportional to polyQ length in PC12 cells stably expressing an inducible htt transgene. Expression of the transgene in stable httQ25GFP and httQ103GFP PC12 cell lines transfected with mRFP was induced with tetracycline and followed for 6 days. Cells expressing httQ103 have a significantly increased risk of death compared to cells expressing httQ25 ($p < 0.001$; $n > 100$, 2 replicates).

PolyQ length and intracellular dosage predict IB formation

In these experiments, some cells that express mutant htt form IBs before they die and some do not. We found that neurons or PC12 cells with httQ97 form IBs more frequently and at a faster rate than those with httQ47 (Fig 2.7), while htt with shorter stretches such as Q17 or Q25 don't form IBs at all.

We then tested whether increased amounts of mutant protein within the cell increases the risk that the cell will form an IB. We have previously demonstrated that fluorescence intensity accurately reflects the amount of diffuse protein present within the cell.¹²⁵ Using Cox proportional hazards analysis, we found a significant association between the amount of intracellular httQ72 protein and the time at which neurons or PC12 cells form IBs.

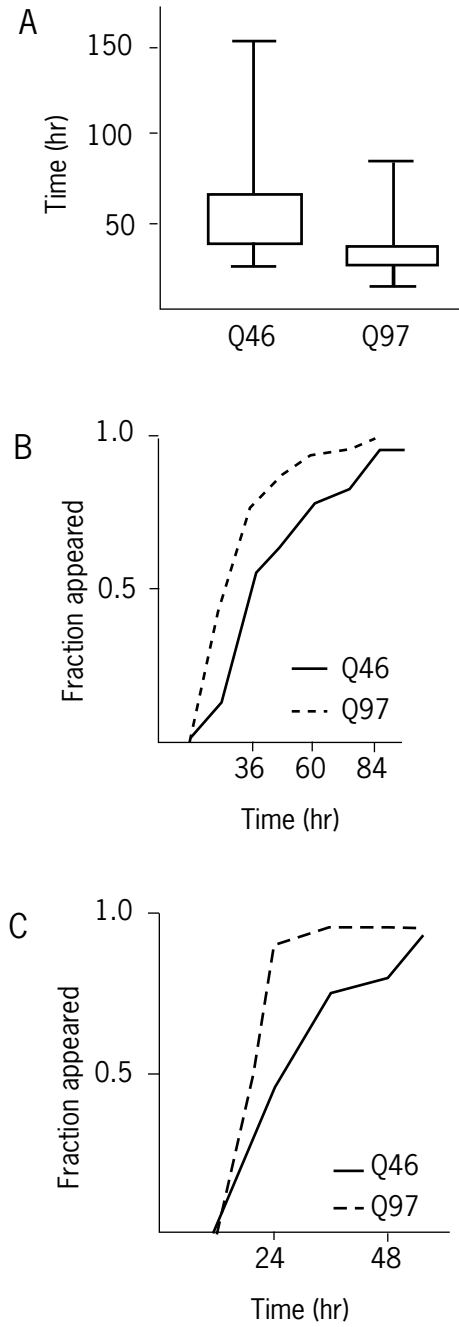


Figure 2.7. IBs form earlier as the polyQ expansion increases. Primary striatal neurons (A,B) and PC12 cells (C) form IBs more slowly when transiently transfected with httQ46 than with httQ97. Box and whiskers (A) and cumulative histograms (B,C) showing the distribution of times of IB formation.

IBs are protective

If the difference in survival between cells expressing short and expanded polyQ tracts was due only to the formation of IBs which were toxic to the cell, we would expect cells with the highest burden of IBs to die fastest. If instead, cells formed IBs as a protective response to toxic protein, we would expect those cells with IBs to survive better than those without.

To distinguish between these possibilities, we determined if cells died faster or slower following IB formation. To perform this analysis, we examined cohorts of cells that formed an IB at a given point in time and compared their survival to parallel cells that never formed IBs. All cells in this comparison survived at least until the point in time at which IB formation was detected to avoid selection bias. We found that both neurons and PC12 cells that formed IBs survived better than those that did not (Fig 2.8).

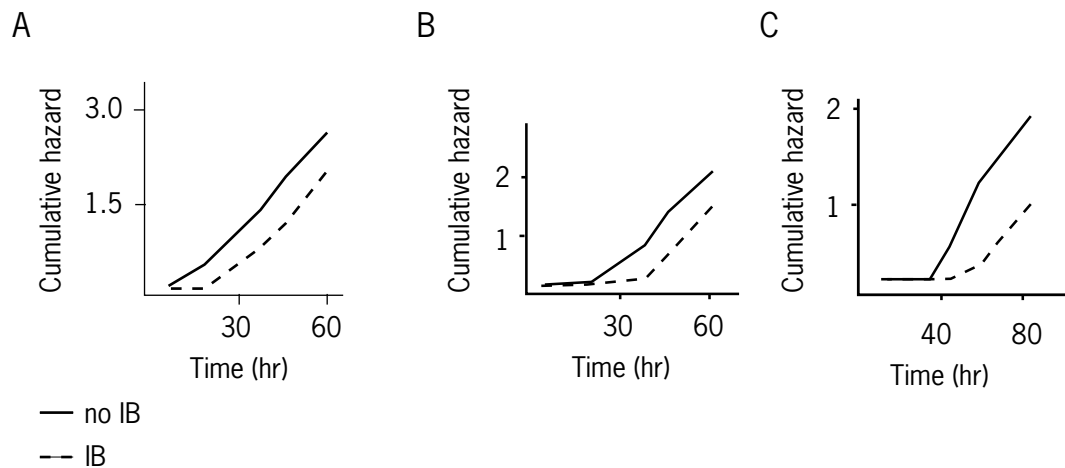


Figure 2.8. Cells that form IBs survive longer than those without. The risk of death for PC12 cells that formed inclusion bodies at 11 (A), 20 (B), and 38 (C) hours after transfection (dotted lines) was less than cells that lived at least 11 (A), 20 (B) and 38 (C) hours but did not form inclusion bodies (solid lines). The comparison was done with matched survival to the point of IB formation to avoid selection bias. ($p < 0.001$, $p < 0.03$, $p < 0.02$)

Diffuse mutant protein is toxic

After determining that cells with IBs survive better than those without, we tested if IB formation was even necessary for increased polyQ-dependent toxicity. We performed a secondary analysis of only those cells that did not form IBs before they died. From experiments where we image as frequently as every two hours, we know that we miss fewer than 2% of the total IBs that form due to cells dying before the IB can be imaged. When we compared only cells that never form IBs, we found the same polyQ-dependent increase in toxicity that we observed with the cells generally. Primary neurons that express httQ46 or httQ97 and never form IBs die faster than those expressing httQ17 or GFP alone (Fig 2.9). Similarly, transiently transfected PC12 cells that never form IBs die faster with httQ47 or httQ97 than with httQ17 and stably-transfected PC12 cells that never form IBs die faster with httQ103 than httQ25 (Fig 2.10).

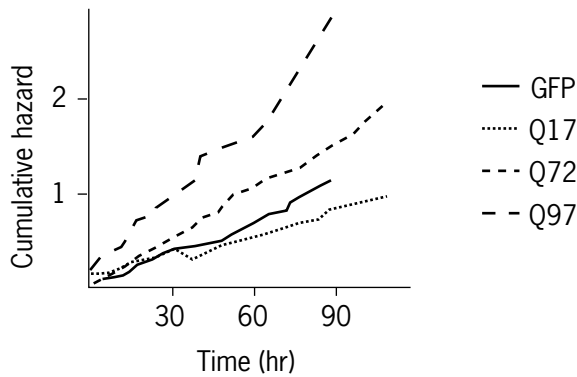


Figure 2.9. IB formation is not required for polyQ dependent toxicity in neurons. Secondary analysis of data from Fig 2.4, comparing cells expressing GFP, httQ17, httQ72 and httQ97 that did not form IBs. Cells with httQ72 that do not form IBs have an increased risk of death compared to httQ17 or GFP ($p < 0.001$). Cells with httQ97 that do not form IBs have the highest risk of death ($p < 0.001$).

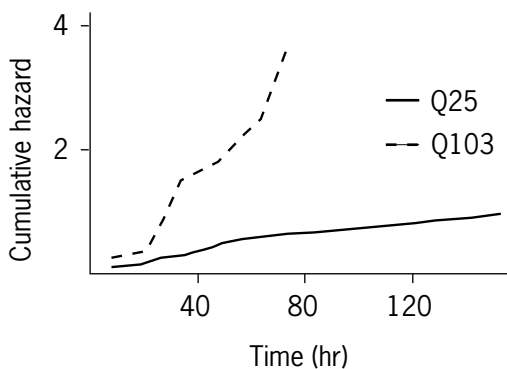


Figure 2.10. IB formation is not required for polyQ dependent toxicity in PC12 cells. Secondary analysis of data from Fig 2.6, comparing httQ25 and only those httQ103 cells that did not form IBs. Cells with httQ103 that do not form IBs have a significantly higher risk of cell death than cells with httQ25 ($p < 0.001$).

IB formation in our primary culture system is marked by a complete loss of diffuse mutant htt from the cell otherwise.¹²⁵ This observation prompted us to examine whether IBs were manifesting a protective effect by sequestering toxic mutant protein. If this was the case, we might expect that the amount of diffuse mutant htt would predict the extent of toxicity. Using Cox proportional hazards analysis, we determined that neurons or PC12 cells (Fig 2.11) with higher intracellular levels of diffuse mutant htt were more likely to die earlier. There was no relationship between levels of either htt with sub-threshold polyQ stretches or fluorescent protein alone and the risk of death.

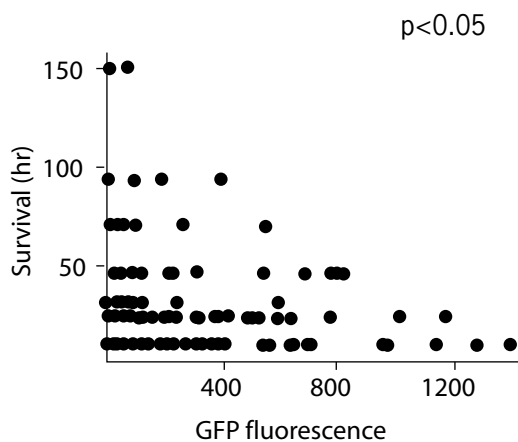


Figure 2.11. Intracellular htt level predicts the duration of cell survival. Individual neurons are plotted by httQ72GFP fluorescence at the first measurement (as a surrogate for mutant htt levels) and the eventual survival of those same cells. Note the lack of cells in the upper right corner. No cells with high mutant htt levels (right side of the graph) survived past 75 hours. Using Cox proportional hazards analysis with mutant htt level as a numerical covariate, a significant association is present between the magnitude of mutant htt levels and the duration of cellular survival. ($p < 0.05$)

Discussion

In this study, we capitalized on the ability of longitudinal single-cell analysis to identify stochastic intracellular processes as they unfold and relate those changes to a cellular outcome. We identified and tracked cells with IBs and found that neurons or PC12 cells that formed IBs survived longer than those that did not. The polyQ-dependent toxicity that we saw did not require IB formation; instead, the amount of diffuse mutant protein with a given polyQ length predicted the survival of neurons and PC12 cells. As higher levels of diffuse mutant protein with a given polyQ length also predicted IB formation and IB formation was accompanied by a reduction in the levels of diffuse mutant protein, our data supports a model where IB formation is protective by sequestering erstwhile toxic protein.

Though our data strongly suggests that inclusion body formation is part of a protective coping response to mutant htt protein, it does not necessitate that IBs themselves are beneficial to the survival of the cell. Though evidence points to IBs as active sites of protein degradation,⁹⁷ it is also apparent that the formation of these structures may be accompanied by an inhibition in that same machinery^{96, 126}. Understanding how the formation of IBs is protecting cells will require a closer examination of the dynamics of the impairment of protein degradation¹²⁷ and whether this impairment is a primary mediator of toxicity. This study raises the intriguing possibility that enhancing IB formation could be a therapeutic avenue for HD and neurodegenerative disease generally.

Aggregating protein and the formation of higher order structures is a common feature of many neurodegenerative diseases. In the case of HD, many smaller aggregated species likely precede the formation of IBs. This study demonstrates that these smaller species are sufficient to explain the toxicity of expanded polyQ tracts. The exact identity of the toxic species and the mechanism by which they are toxic remains to be shown.

Our results shift the focus onto those species to understand how cellular pathogenesis progresses and design therapeutics to improve neuronal function and survival in HD.

Materials and Methods

Plasmids

The pGW1-httQ17-eGFP mammalian expression plasmid was created by PCR from GFP-109-17Q-Bgal (Dr. R. Truant, McMaster University, Ontario, Canada) with flanking XhoI/BamHI sites that was subcloned through pcDNA3.1 into pGW1 using KpnI/XbaI. An expression plasmid encoding an exon 1 fragment of htt with 97 glutamines fused to eGFP in pGW1 (British Biotechnologies) was subcloned from a construct in pcDNA3 (Dr. D. Housman, MIT, Cambridge, MA) by digestion with AgeI, a Klenow reaction to fill in the overhang, digestion with KpnI and ligation into the KpnI/NruI sites of the pGW1 vector. The expression plasmids encoding an exon 1 fragment of htt with 25, 46, and 72 glutamines fused to eGFP in pGW1 were created by replacement of httQ97 with a KpnI/XbaI fragment from analogous constructs in pcDNA3 (Dr. D. Housman, MIT, Cambridge, MA). mRFP1 was subcloned from pRSETB-mRFP1 (R. Tsien, UCSD, San Diego, CA) into pcDNA3.1(+) using BamHI/EcoRI and then into pGW1 using HindIII/EcoRI. Enzymes used for cloning were from New England Biolabs (Beverly, MA).

Cell culture

Wild-type PC12 cells or PC12 cells stably expressing httQ25-eGFP and httQ103-eGFP under an ecdysone inducible promoter (E. Schweitzer, UCLA, Los Angeles, CA) were plated at 10^4 cells per cm^2 in 24-well tissue culture plates coated with high molecular weight Poly-D-Lysine (BD Biosciences, San Jose, CA). Cells were grown in high glucose DMEM (Mediatech, Herndon, VA) with 5% supplemented calf serum (Hyclone, Logan, UT), 5% equine serum (Hyclone, Logan, UT), L-glutamine (Invitrogen, Carlsbad, CA)

and Penicillin-Streptomycin (Invitrogen, Carlsbad, CA) in a 9.5% CO₂ incubator at 37°C. Media was changed every two-three days.

Primary cultures of rat striatal neurons were prepared from embryos following 16-18 days of gestation as described previously.^{121, 128} Briefly, striata were dissected in ice-cold DM/KY: dissociation medium (81.8mM Na₂SO₄, 30mM K₂SO₄, 15.2mM MgCl₂, 0.25mM CaCl₂, 1mM HEPES pH 7.4, 20mM glucose, and 0.001% phenol red) supplemented with 1mM Kynurenic acid (Sigma-Aldrich, St. Louis, MO). 10U/ml papain (Worthington Biochemical, Lakewood, NJ) was preincubated with 0.42mg/ml L-cysteine (Sigma-Aldrich, St. Louis, MO) in DM/KY in a 37°C water bath for 20-30 minutes. The tissue was then treated with the activated papain in two serial incubations of 15 minutes each at 37°C. The papain was removed by three washes of five minutes each at 37°C with 10mg/ml Trypsin Inhibitor (Sigma-Aldrich, St. Louis, MO) in DM/KY. The tissue was triturated to single cells in Optimem (Invitrogen, Carlsbad, CA) supplemented with 20mM glucose. Cells were counted with Trypan blue, and plated at 5.8x10⁵ cells per well in 24-well tissue culture plates coated with HMW Poly-D-Lysine and Laminin (BD Biosciences, San Jose, CA). Two hours later, media on the cells was replaced with 1 ml of modified neuronal culture medium (NCM), a basal medium of Eagle (Invitrogen, Carlsbad, CA) based growth medium containing serum (formulation available at <http://www.gladstone.ucsf.edu/gladstone/files/finkbeiner/Protocols/cprotocol.pdf>). Cells were fed every five-seven days by washing three times in basal medium of Eagle and replacement with equal measures of conditioned and fresh neuronal culture medium.

Transfection

24 hours after plating, PC12 cells were transfected with pcDNA3.1(+)-mRFP and pGW1-httQ17,25,46,72,97-eGFP (wild-type) or transfected with mRFP alone and induced with 1μM tebufenozide (stables) (Fred Gage, La Jolla, CA). Plasmids were

transfected in a 1:1 molar ratio with 2 μg total DNA per well. Cells were washed three times with DMEM and allowed to equilibrate for 30 minutes at 37°C/9.5% CO₂. Calcium phosphate and plasmid solution was added dropwise to 2xHEPES buffered saline and precipitate was allowed to develop for 15 minutes in the dark. Calcium phosphate precipitate was added dropwise to PC12 cells and the cells were incubated 15-30 minutes at 37°C/9.5% CO₂ to allow precipitate to develop. After washing the cells three times with DMEM, growth media containing serum was returned to the cells.

Primary cultures were transfected 5-7 days in vitro with pcDNA3.1(+)-mRFP and pGW1-httQ(17, 25, 46, 72, 97)-eGFP or pGW1-eGFP alone in a 1:1 molar ratio with 2-3 μg total plasmid DNA per well. Primary neurons were washed three times in DMEM supplemented with 10mM Kynurenic acid (DMEM/KY) and incubated at 37°C/9.5% CO₂ for 30 minutes prior to transfection. Calcium chloride and DNA solutions were added dropwise to 2xHBS. Calcium phosphate precipitate was allowed to develop in the dark for 10-15 minutes and then added to the cells dropwise. Precipitate on the cells was allowed to develop between 15-30 minutes depending on the rate at which precipitate formed. Cells were treated with an osmotic shock solution (2% DMSO (Fisher Scientific, Fairlawn, NJ), 5% DM/KY in hepes buffered saline) for 1-2 minutes, washed twice with DMEM/KY, once with basal medium of Eagle, and the media was replaced with 1 ml of a 1:1 combination of conditioned and fresh NCM.

Live-cell imaging and analysis

The imaging was performed with a Nikon TE300 inverted microscope mounted on a vibration isolation table (Technical Manufacturing, Peabody, MA) using a long working-distance Nikon 20X (NA 0.45) objective. Images were detected and digitized using a Hamamatsu Orca II camera with a 12-bit/14-bit digital cooled charge-coupled device detector (Hamamatsu Photonics, Bridgewater, NJ). Stage movements and focusing were

performed using a Proscan II stage controller (Prior Scientific, Rockland MA). Samples were illuminated with a 175W Xenon Lambda LS illuminator (Sutter Instruments, Novato, CA) with liquid light guide and fluorescence excitation and emission filters were placed into the light path using a computer-controlled Lambda 10-2 controller and two ten-position filter wheels (Sutter Instruments, Novato, CA). GFP and RFP images were captured using an 86014 beamsplitter and 480/40x;517/30m and 580/20x;630/60m fluorescence filters (Chroma Corp, Rockingham, VT) respectively. Algorithms for plate registration, stage movements, filter movements, focusing and acquisition were generated with Metamorph imaging software (MDS, Inc, Mississauga, Ontario, Canada). Thirteen images per fluorescence channel were captured per well and analyzed manually using Metamorph software. Survival analysis was performed with the Statview software package (SAS Institute, Cary, NC) and other statistical analysis was performed with Prism (Graphpad Software, San Diego, CA).

Chapter 3: Understanding the role of the ubiquitin-proteasome system in the pathogenesis of Huntington's disease

Abstract

The accumulation of mutant protein in intracellular aggregates is a common feature of neurodegenerative disease. In Huntington's disease, huntingtin protein with a polyglutamine expansion triggers intracellular aggregation into inclusion bodies and neuronal toxicity. Due to the accumulation of mutant protein, impairment of intracellular protein degradation and particularly the ubiquitin-proteasome system have been implicated in the pathogenesis of Huntington's disease. The relationship between inclusion body formation and ubiquitin-proteasome function has been difficult to establish due to the asynchronous formation of inclusion bodies in a subset of cells affected by the disease. Here, we have applied a single-cell longitudinal acquisition and analysis platform to monitor inclusion body formation, ubiquitin-proteasome system function, and neuronal toxicity. We find that proteasome inhibition is toxic to striatal neurons in a dose-dependent fashion. Preceding inclusion body formation, neurons that later form inclusion bodies have higher levels of ubiquitin-proteasome system impairment when compared to those that do not form inclusion bodies. After forming inclusion bodies, however, neurons have lower levels of ubiquitin-proteasome system impairment compared to non-inclusion body forming cells. Our findings support a model where inclusion bodies are a protective cellular response to mutant protein mediated in part by improving intracellular protein degradation.

Introduction

Huntington's disease (HD) is a progressive neurodegenerative disorder without a cure. The expansion of a polyglutamine (polyQ) stretch in the amino-terminal end of the huntingtin protein (htt) above a threshold length of 36 causes the disease. PolyQ expansions within proteins in the nervous system cause a series of different neurodegenerative disorders.²⁷ Most polyQ disorders are dominantly inherited, supporting a hypothesis that the mutant polyQ-containing proteins confer a toxic gain of function.¹¹¹

As with other polyQ diseases, the cellular pathogenesis of HD is accompanied by the development of deposits of aggregated mutant protein called inclusion bodies (IBs), detectable in human post-mortem samples,⁷⁰ transgenic mouse brain,⁷¹ and cell culture models.¹²¹ We have previously examined the relationship between htt, IBs, and neuronal toxicity and found that mutant htt induced neuronal toxicity in a dose-dependent manner. Not only were IBs not required for mutant htt toxicity, cells that developed IBs survived better than those that did not. If IB formation is accompanied by improved cellular survival, mutant htt must mediate neurodegeneration through a different mechanism.

The accumulation of ubiquitinated proteins in IBs in ALS, Parkinson's disease, and polyQ-mediated disorders has implicated the degradation of proteins by the ubiquitin-proteasome system (UPS) in the pathogenesis of these neurodegenerative diseases. The UPS is a major pathway for the degradation of intracellular protein.^{129, 130} To target proteins for degradation, ubiquitin, a 76 amino acid polypeptide, forms sequential thioester linkages with cysteine residues on E1 ubiquitin activating enzymes and E2 ubiquitin conjugating enzymes and, with the assistance of a ubiquitin ligase, forms an isopeptide bond with the amino group of lysine residues on the substrate.⁹⁴ Several internal lysine residues within ubiquitin can then be used as sites for additional ubiquitin addition. Once a protein is modified by a polyubiquitin chain with a minimum of four ubiquitins, the

protein is efficiently targeted to the proteasome for degradation. The proteasome itself is a multicatalytic complex consisting of a 19S regulatory subunit and 20S core that contains chymotrypsin-like, trypsin-like, and post-glutamyl peptidase activities.⁹⁵

Inhibition of the proteasome in proliferating cells causes cell cycle arrest and ensuing cell death. In neurons, proteasome inhibition may lead to cell death through an accumulation of signals for apoptosis, a decrease in NF- κ B signaling, sensitization to other toxic stimuli, remodeling of synapses, retraction of neurites, or through other unidentified mechanisms.^{131, 132} The effect of proteasome inhibition is cell-type and cell-cycle dependent and the relationship between proteasome inhibition and striatal neuronal survival is largely unknown.

Proteasome inhibition may be one mechanism through which diffuse mutant htt is toxic. Since mutant htt forms IBs in a polyQ and protein concentration dependent manner, a central challenge in assessing the effect of diffuse mutant htt is the propensity of this protein to form IBs in a subset of cells expressing mutant htt. Though analyzing populations of mutant htt-expressing cells has been complicated, it is clear that IB formation is not required for UPS impairment.^{127, 133}

The relationship between IB formation and UPS function remains unresolved. Proteasome subunits and heat shock proteins colocalize with IBs, but it is unclear if this colocalization is beneficial, facilitating protein delivery or unfolding proteins at the mouth of active proteasomes, or if it is detrimental, functionally sequestering essential cellular machinery.^{78, 134, 135} A number of studies indicate that protein turnover in cells with IBs is reduced, accompanied by the accumulation of cellular proteins.^{117, 136, 137} HEK293 cells containing mutant htt IBs have increased levels of proteasome impairment relative to those cells without IBs.⁹⁶ Some studies show that htt IBs are relatively static.^{99, 138} However, protein in IBs of other aggregate-prone proteins are dynamically exchanged with cytoplasmic and nuclear pools and protein turnover within IBs may be accelerated;^{97, 139} if

this is the case, then cells with IBs may have an increased capacity for protein degradation.

Interpretation of these studies is complicated by the inability to determine which events precede others. As an example, the observation that cells with IBs have impaired UPS function does not allow us to determine if IB formation leads to UPS inhibition or if UPS inhibition leads to IB formation. If proteasome inhibition leads to IB formation and prolonged cell survival, this would support a hypothesis that IB formation is a beneficial coping response of the cell; if instead, IB formation leads to proteasome inhibition, this would support a toxic function for IB formation. Furthermore, as IB formation is not a universal event in all cells expressing mutant htt, determining the effect of IBs on toxicity in a population of cells expressing mutant htt is confounded by the fact that some cells express only diffuse mutant htt throughout the course of their lives.

To overcome these obstacles, we have applied a single-cell longitudinal approach to gain spatial and temporal resolution and simultaneously visually monitor IB formation, UPS inhibition, and neuronal toxicity. We found that proteasome inhibition is toxic to primary striatal neurons in a dose-dependent fashion. UPS inhibition is higher in those cells that will go on to form IBs, but is reduced following IB formation. As cells that form IBs survive longer than those that do not, our results support the conclusion that IB formation may be protective by improving UPS function.

Results

Single-cell longitudinal analysis of ubiquitin-proteasome function in primary neurons

To monitor dynamic changes in protein degradation in live cells, we employed a novel high-throughput image acquisition platform we have described previously^{122, 125} and fluorescent protein substrates of ubiquitin-proteasome system (UPS) degradation. We targeted fluorescent proteins to the UPS for degradation by the addition of either the CL1 peptide tag¹⁴⁰ to the carboxy-terminus or a non-hydrolyzable ubiquitin moiety (Ub^{G76V})¹⁴¹

to the amino-terminus. These destabilized fluorescent proteins were then transfected into primary neurons and fluorescence in individual cells was monitored over the course of days to detect changes in the degradation of UPS substrates. To simultaneously monitor cell survival¹²⁵ and control for nonspecific changes in transcription and protein handling, we co-transfected and tracked the fluorescence of unmodified fluorescent proteins in the same cells.

In order to validate destabilized fluorescent proteins as reporters of the UPS in primary striatal neurons, we examined changes in reporter fluorescence in response to pharmacological inhibition of the proteasome. Previously, we have shown that measurements of fluorescence intensity in live cells is an accurate indicator of the amount of fluorescent protein present within the cell.¹²⁵ We found that fluorescence levels in primary striatal neurons of a destabilized form of enhanced green fluorescent protein (GFP^u)⁹⁶ increased after treatment with the proteasome inhibitor MG132, even when we controlled for changes in fluorescence of unmodified monomeric red fluorescent protein 1¹²⁴ (mRFP) in the same cells (Fig 3.1).

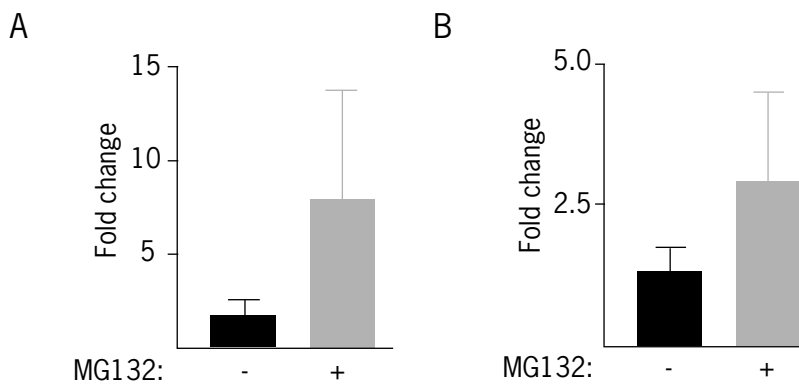


Figure 3.1. Levels of GFP^u increase following MG132 treatment. Following transfection with GFP^u and mRFP, striatal neurons were treated with 50 μ M MG132 for 12 hours. GFP fluorescence (A) and the ratio of GFP/mRFP fluorescence (B) both increase after MG132 treatment relative to control.

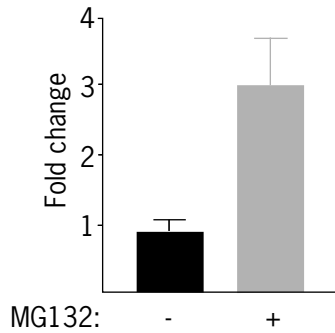


Figure 3.2. Levels of mRFP^u increase following MG132 treatment. Following transfection with mRFP^u and GFP, neurons were treated with 50 μ M MG132 for 12 hours. The mRFP^u/GFP ratio is significantly increased relative to control.

Similarly, treatment of neurons with MG132 increased the levels of a destabilized form of the mRFP protein (mRFP^u) even when levels of unmodified GFP in the same cells were taken into account (Fig 3.2). Levels of two different destabilized forms of the enhanced yellow fluorescent protein variant Venus¹⁴² (Ub^{G76V}-Venus and Venus^u) were both increased by treatment of neurons with the specific proteasome inhibitor epoxomicin, even when Venus levels were normalized to levels of unmodified cyan fluorescent protein (CFP) in the same cells (Fig 3.3). Low basal levels combined with a significant, rapid increase in fluorescence after proteasome inhibition established the fluorescence of these reporters as an indication of UPS impairment in primary neurons, in agreement with previously published reports of their use in cell lines.^{96, 127, 133}

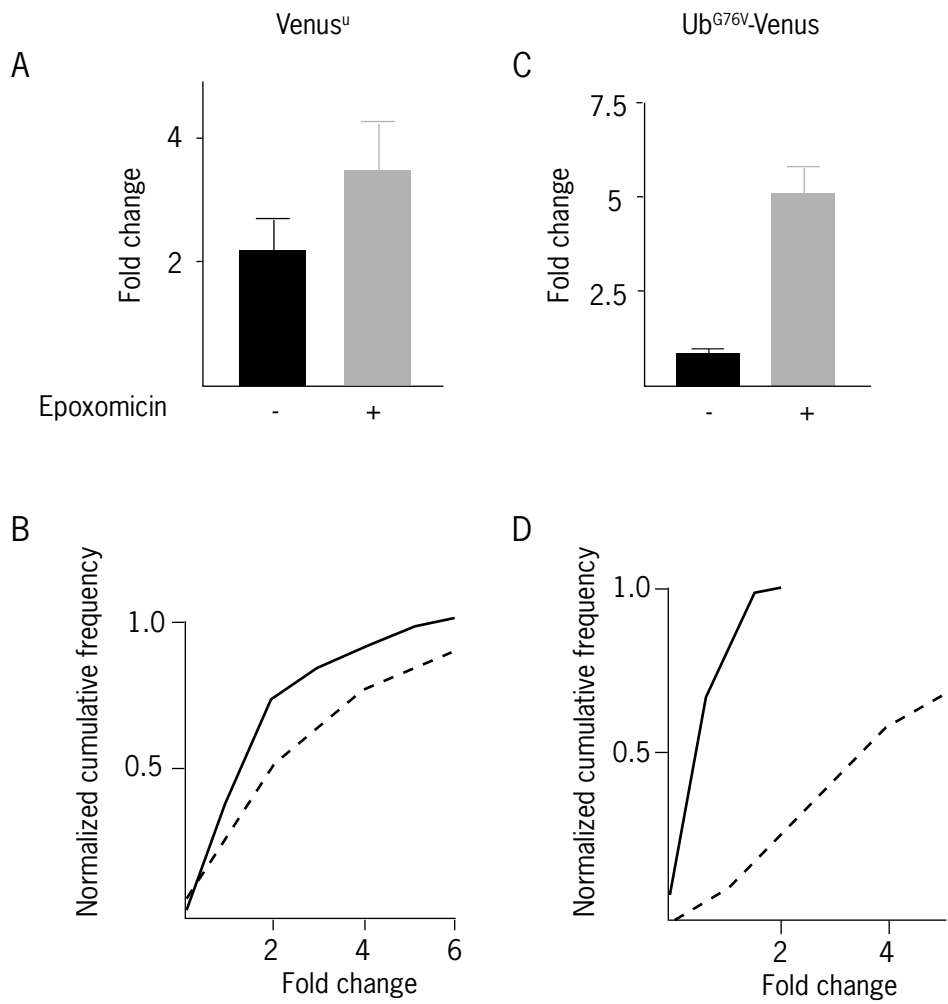


Figure 3.3. Levels of Venus^u and Ub^{G76V}-Venus increase following epoxomicin treatment. Following transfection with CFP and Venus^u (A,B) or CFP and Ub^{G76V}-Venus (C,D) neurons were treated with 2 μ M epoxomicin for 10 hours. Both mean change in Venus/CFP fluorescence (A,C) and single cell distributions of Venus/CFP fluorescence (B,D) are significantly increased relative to control.

UPS reporters do not respond to inhibition of macroautophagy

To ensure that these destabilized proteins were targeted primarily to the UPS for degradation, we examined their response to the pharmacological inhibition of autophagy. Bafilomycin A1 (Baf A1) is a vacuolar ATPase inhibitor¹⁴³ that prevents autophagosome-lysosome fusion and causes the accumulation of substrates targeted for macroautophagy.¹⁴⁴ We observed that though BafA1 caused a rapid accumulation of LC3-II and was clearly toxic to primary neurons, BafA1 treatment did not lead to increases in the levels of UPS reporters (Fig 3.4).

Proteasome inhibition is not sufficient to induce macroautophagy in primary neurons

Though autophagy does not routinely handle UPS reporters, it is possible that proteasome impairment could induce the upregulation of autophagic activity to degrade accumulating proteins. To test this possibility, we examined the activity of the autophagic pathway following proteasome inhibition. The level of activated LC3 (LC3-II) is commonly used as a surrogate for the number of autophagosomes and flux through the macroautophagic pathway.¹⁴⁵ After treatment with epoxomicin, primary neurons show no change in LC3-II levels (Fig 3.4). Since BafA1 has no effect on UPS reporter accumulation and flux through the autophagic pathway is unchanged following proteasome inhibition, it is unlikely that autophagic activity has a significant effect on UPS reporter levels.

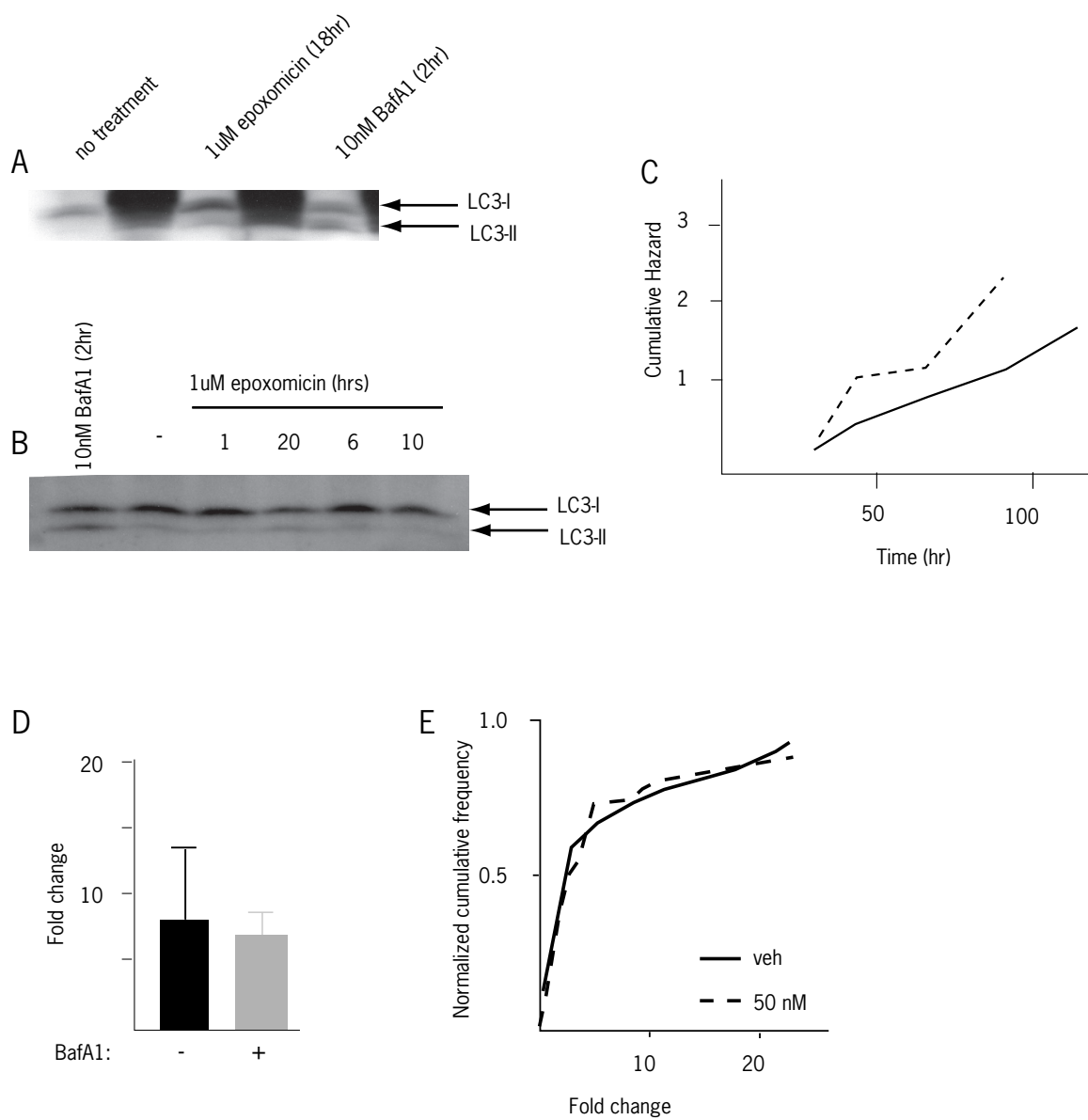


Figure 3.4. Limited interaction between the UPS and autophagic pathways in neurons. Data in (A) and (B) were generated by A. Tsvetkov. Cells were treated with either BafA1 or epoxomicin. Following treatment, western blotting was performed on cell lysates with an LC3 antibody. While BafA1 caused an accumulation of LC3-II in both HEK293 cells (A) and neurons (B), epoxomicin changed LC3-II levels in HEK293 cells (A) but not in neurons (B). In parallel experiments (C), 24 hours after transfection with CFP and Ub^{G76V}-Venus, neurons were treated with vehicle or 50nM BafA1. BafA1 treatment caused a significant amount of toxicity above control ($p < 0.03$). Mean Venus/CFP ratio (D) and the distribution of single cell changes in Venus/CFP (E) in these cells did not increase above control in the 20 hours following BafA1 addition.

Neuronal toxicity is proportional to the extent of proteasome inhibition

After determining that UPS reporters responded to proteasome inhibition in primary neurons, we then examined the nature of their response to varying levels of proteasome impairment. We co-transfected mRFP^u and GFP into primary striatal neurons and treated the cells with increasing doses of MG132. As early as 2.5 hours after addition of MG132, we saw increases in reporter fluorescence and the magnitude of the increase was proportional to the amount of MG132 added (Fig 3.5). Reporter fluorescence continued to increase as additional time elapsed, again in a MG132 dose-dependent fashion (Fig 3.6). This response indicated that not only do the reporters respond to proteasome impairment,^{96, 127} but that the increase in their fluorescence is proportional to the extent of proteasome impairment in primary neurons.

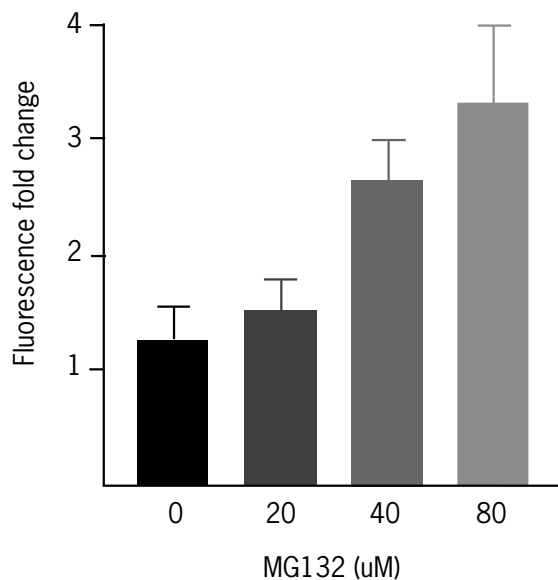


Figure 3.5. UPS reporter fluorescence shows a dose dependent response to MG132 treatment. MG132 at the indicated doses was added to striatal neurons 24 hours following transfection with mRFP^u and GFP. The change in mRFP^u/GFP ratio over the first 2.5 hours following MG132 administration is shown.

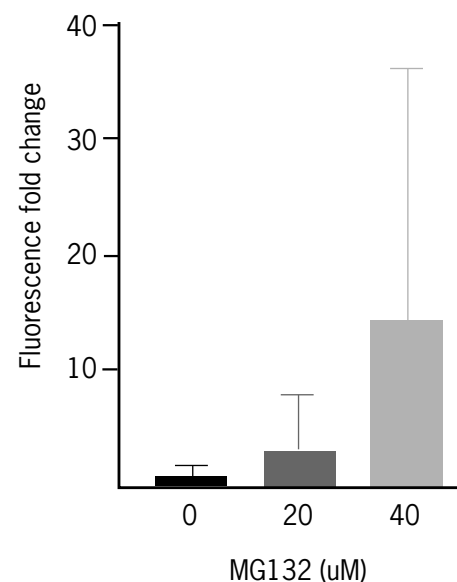


Figure 3.6. UPS reporter fluorescence continues to increase up to 12 hours after the addition of MG132. Note the difference in scale with Fig 3.5. The change in mRFP^u/GFP ratio over the 12 hours following MG132 administration is shown. Measurements from 80mM treatment with MG132 were excluded due to noticeable toxicity in the treated cells.

By monitoring individual cells treated with increasing doses of MG132 over the course of days, we determined the effect of increasing proteasome inhibition on the survival of primary striatal neurons. When the dose of MG132 increased, neurons died faster (Fig 3.7). As these are the same neurons that show an increase in reporter fluorescence after treatment with MG132, we found a proportional relationship between proteasome impairment and both the accumulation of UPS substrates and the resulting neuronal toxicity.

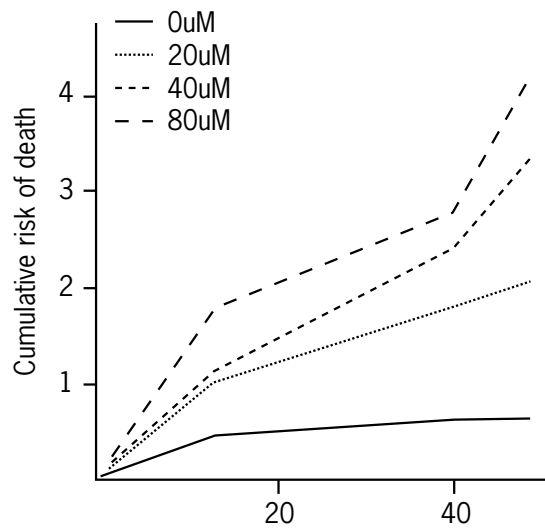


Figure 3.7. MG132 is toxic to neurons in a dose-dependent fashion. The same neurons analyzed in Figs 3.5 and 3.6 were observed for 5 days with hazard functions shown. 20 μ M, 40 μ M, and 80 μ M MG132 show graded increases in toxicity when compared to treatment with vehicle.

Dynamic changes in UPS function in a primary striatal model of HD

The cellular pathogenesis of HD is marked by both the development of IBs^{70, 71} and impairment of the proteasome.^{96, 127, 146} Though IBs are not required for htt-dependent proteasome impairment,^{127, 133} it remains unclear what triggers these structures to form and what effect IB formation has on intracellular protein degradation. As it has not been possible to predict which cells will form IBs, our high-throughput longitudinal single-cell imaging platform¹²² offered an opportunity to identify neurons that did or did not form IBs in an unbiased fashion without the need for manipulations that may change the biology of the system.

We used a previously characterized primary striatal model of HD¹²¹ and prospectively followed visual markers of UPS function, IB formation and neuronal viability. Our primary neuronal model reproduces key features of HD, including neuronal subtype specificity¹²¹ and polyglutamine length dependent toxicity.^{121, 125} To induce the HD disease phenotype in this model, we transiently transfected an amino-terminal htt fragment incorporating 72 glutamines fused to GFP (htt^{ex1}Q72-GFP). A similar N-terminal fragment is present in HD brain⁶⁸ and is sufficient to cause progressive neurodegeneration resembling HD in mice.^{71, 59} We simultaneously introduced mRFP^u and blue fluorescent protein (BFP) into the same neurons to monitor UPS impairment and cell viability, respectively. After transfection, we imaged the cells at 8-24 hour intervals (Fig 3.8). Though experiments in cell lines sometimes demonstrate a relocalization of fluorescent UPS reporters to IBs,¹²⁷ we find that mRFP^u remains diffusely fluorescent throughout the neuron in our experiments.

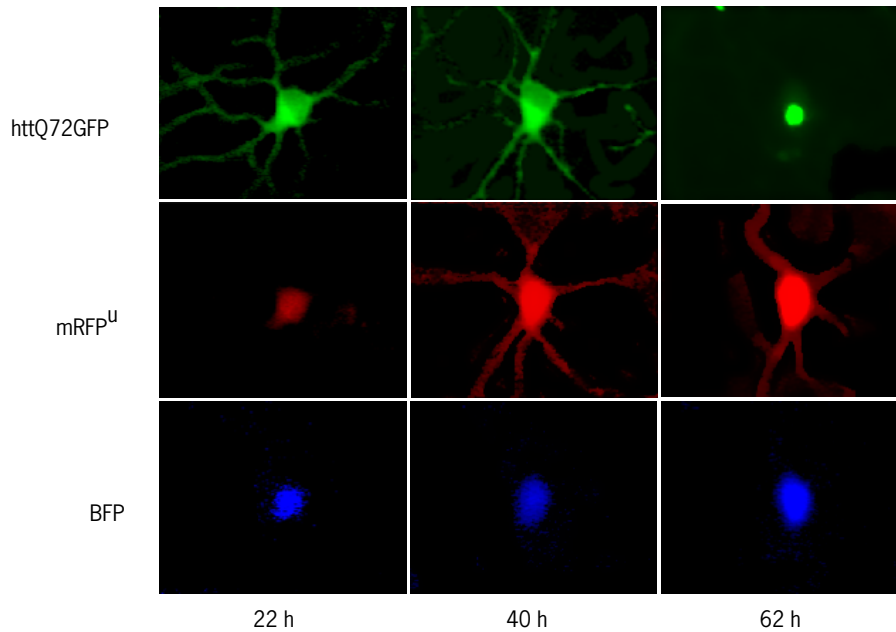


Figure 3.8. Three color longitudinal imaging of primary neurons in culture. GFP, mRFP^U and BFP were sequentially imaged over the course of days to follow htt IB formation, UPS impairment and neuronal survival, respectively.

Proteasome impairment precedes IB formation

From series of images of individual neurons, we quantified single-cell changes in UPS reporter fluorescence over the course of the lives of cells expressing the htt^{ex1}Q72-GFP protein. We were particularly interested in whether neurons that would go on to form IBs differed in UPS function from those that would never form IBs. To compare cohorts of neurons that did or did not form IBs without cell survival as a confound, we compared neurons that never formed IBs but survived at least as long as the time of IB formation of their counterparts that did form IBs.

One such comparison is between neurons expressing htt^{ex1}Q72-GFP that formed IBs 54 hours after transfection and neurons that survived at least 54 hours but never formed IBs. Those cells that would go on to form IBs at 54 hours had significantly larger increases in UPS reporter fluorescence preceding IB formation, both in mean reporter fluorescence and in the single-cell distribution of reporter fluorescence, than their non-IB

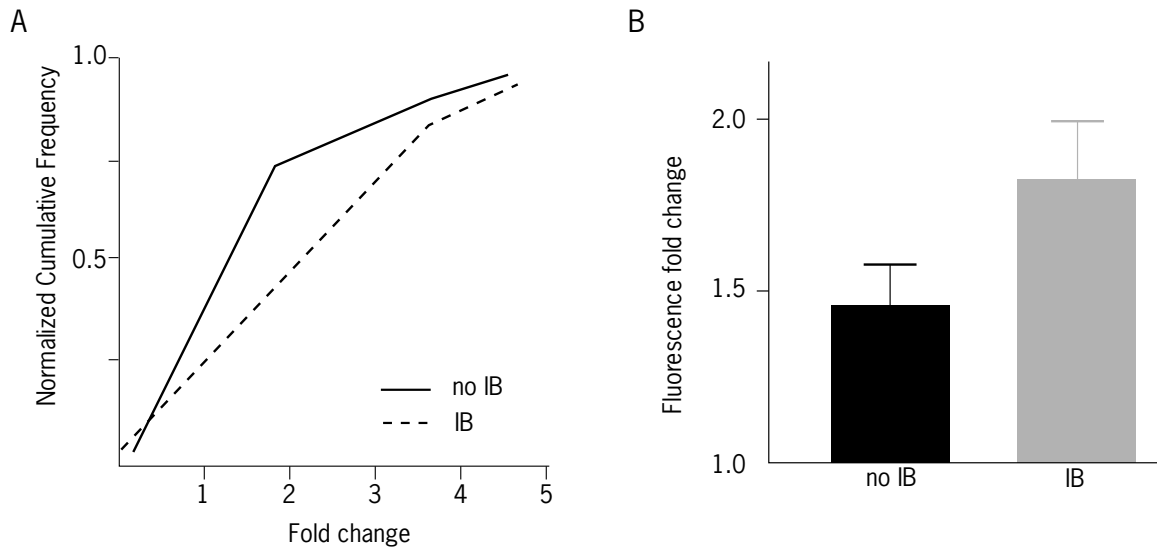


Figure 3.9. UPS impairment precedes IB formation at 54 hours after transfection. Single-cell distributions (A) or population means (B) of the change in mRFP^v/GFP fluorescence in the interval preceding IB formation. The increase in mRFP^v/GFP ratio was higher in cells that went on to form IBs ($p < 0.02$).

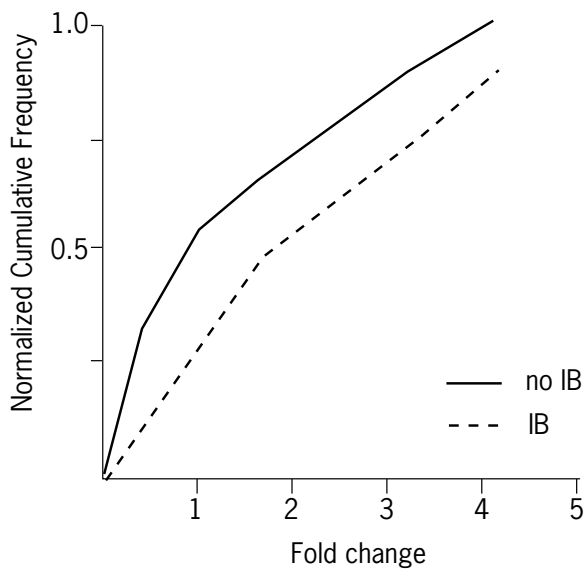


Figure 3.10. UPS impairment precedes IB formation at 76 hours after transfection. Single-cell distributions of change in mRFP^v/GFP ratio in the interval preceding IB formation show higher UPS impairment in those cell that will go on to form IBs.

forming compatriots (Fig 3.9). Similarly, those cells that would go on to form IBs 76 hours after transfection had larger increases in UPS reporter levels preceding IB formation than those cells that survived at least that long but never formed IBs (Fig 3.10). More generally, we found that those neurons that formed IBs had higher UPS impairment preceding IB formation than those that did not form IBs.

Proteasome impairment decreases following IB formation

We also performed analogous analysis to examine UPS reporter fluorescence following IB formation. Here, we were interested in testing whether IB formation improves or worsens UPS function. To avoid confounding effects of cell survival in our analysis, we compared cohorts of neurons that formed IBs at a given point in time and neurons that did not form IBs; only cells in both groups that survived through the interval following IB formation were analyzed.

When we examined UPS reporter fluorescence in the interval following IB formation, we found that neurons that had formed IBs had significantly lower increases in UPS reporter fluorescence when compared with neurons that had not formed IBs (Fig 3.11). As UPS reporter fluorescence is an indication of the impairment of intracellular protein degradation, we found that UPS impairment was less in cells following IB formation than in cells that did not form IBs.

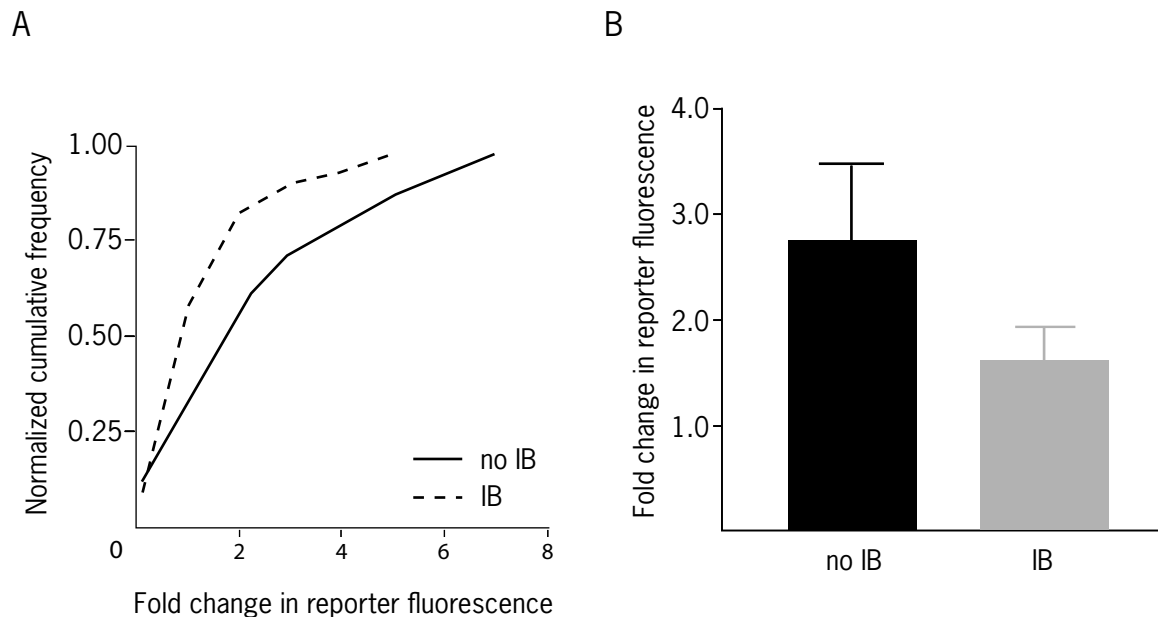


Figure 3.11. An improvement in UPS function follows IB formation. Single-cell distributions (A) and population means (B) representing the change in mRFP⁺/GFP ratio in the interval following IB formation at 54 hours after transfection. The opposite relationship from that in Fig 3.9 and 3.10 is observed.

Neurons that form IBs survive better than those that do not

To determine if this relative improvement in UPS impairment related to neuronal survival, we compared the survival of neurons that we analyzed for UPS function. When we examined neurons transfected with $htt^{ex1}Q72$ -GFP, mRFP^u, and BFP that formed IBs 18 hours after transfection and those that survived at least 18 hours but never formed IBs, we found that those cells that formed IBs survived longer (Fig 3.12). Similarly, those neurons that formed IBs 27 hours after transfection survived better than those neurons that survived at least 27 hours but never formed IBs (Fig 3.13). This is in agreement with previous results in this cell culture model showing that neurons survive better if they form IBs than if they do not.¹²⁵

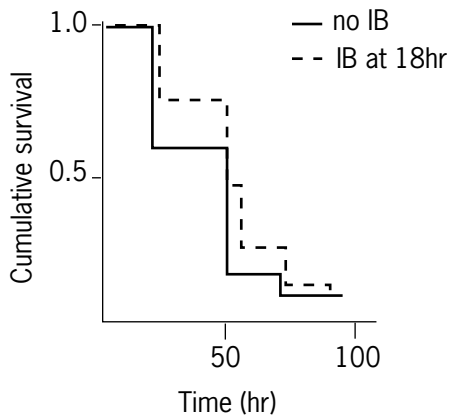


Figure 3.12. Neurons that form IBs at 18 hours post-transfection survive longer than those that do not form IBs. The survival of those neurons that formed htt IBs at 18 hours was better than the survival of neurons that survived at least 18 hours but never formed IBs ($p < 0.01$).

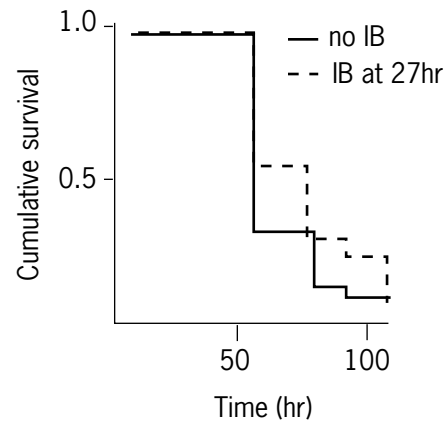


Figure 3.13. Neurons that form IBs at 27 hours post-transfection survive longer than those that do not form IBs. The survival of neurons that formed htt IBs at 27 hours was better than the survival of neurons that survived at least 27 hours but never formed IBs ($p < 0.01$).

Discussion

By applying a high-throughput single-cell imaging platform to a neuronal model of HD, we were able to examine events in the cellular pathogenesis of HD with improved sensitivity and temporal resolution. Through the use of spectrally distinct fluorescent species, we were able to simultaneously monitor neuronal viability, htt IB formation, and intracellular protein degradation. We found that neurons that form IBs have increased proteasome impairment preceding IB formation and decreased proteasome impairment following IB formation when compared to cells that don't form IBs. Though we showed that proteasome inhibition is toxic to primary striatal neurons, the cells that formed IBs survived better than those that did not. In total, these results support a model where IB formation is a protective cellular response to mutant protein and one of the ways this response may improve neuronal survival is by decreasing impairment of UPS function.¹⁴⁶

As of yet, it is unclear how IB formation is functionally linked to an improvement in UPS function. One possibility is that IBs function primarily to sequester mutant protein that otherwise would impair the UPS. There has been some controversy regarding this hypothesis since components of the UPS including ubiquitin and proteasome subunits are present in IBs.^{78, 97-99, 138} Though ataxin-1 and SOD1 IBs have both fast and slow exchanging components,^{97, 98} FRAP and FLIP experiments point to static htt IBs in cell culture.^{99, 138} As these studies were mostly done in cell lines, it is possible that handling of aggregate-prone protein is different in primary neurons, perhaps due to differences in the intracellular milieu of post-mitotic cells.

Another potential explanation for the improvement in UPS function following IB formation could be that aggregation-prone proteins normally targeted to the UPS are shunted to other pathways of intracellular protein degradation once they form an IB. The autophagic pathway of protein degradation is clearly implicated in the clearance of mutant

protein including mutant htt^{105, 147-152} and autophagic machinery is localized to IBs.⁸³ As expanded polyglutamine tracts are largely resistant to eukaryotic proteasomal degradation and may impair the ability of the proteasome to degrade other cellular proteins,¹⁵³ shifting polyglutamine degradation from the UPS to the autophagic pathway could function to increase the flux of other proteins through the UPS. Determining if this is indeed the case will be greatly assisted by experiments examining the half-life of mutant htt preceding and following IB formation with selective inhibition of one or the other pathway of intracellular protein degradation.

Though multiple pathways of intracellular protein degradation may handle aggregation-prone protein,¹⁵⁴ we found that some proteins are likely targeted primarily to the UPS for degradation. Reporters derived from fluorescent proteins allowed us to dynamically monitor UPS function in live cells over time and we found little evidence that they are routinely degraded by autophagy. We found that the UPS reporters do not accumulate when autophagy is inhibited. Though it is clear that autophagy modulates turnover and toxicity of aggregation-prone proteins, addition of the CL1 and Ub^{G76V} degrons do not cause fluorescent proteins in neurons to aggregate. This is in contrast to reports in cell lines¹⁵⁵; the discrepancy may be explained by lower expression levels in neurons relative to cell lines following transient transfection. No matter what the cause, it does not appear that the Ub^{G76V} or CL1 sequences are sufficient to cause a significant amount of protein to be targeted to the autophagic pathway in primary neurons.

The finding that proteasome inhibition is not sufficient to change the flux through the autophagic pathway in primary neurons also highlights differences between mammalian neurons and other model systems. In cell lines,^{108, 156} or *Drosophila melanogaster* eye,¹⁰⁹ proteasome inhibition is sufficient to cause increased autophagosome formation. The difference in behavior of the autophagic pathway in mammalian neurons may be due to differences in constitutive activity.¹⁵⁷ While most cell types show

induction of autophagy following 24 hours of starvation, neurons do not even after 48 hours, ostensibly because constitutive levels of activity are already high.¹⁵⁸ Furthermore, eliminating autophagy results in a neurodegenerative phenotype, emphasizing the importance of constitutive autophagy to neuronal function and survival.^{103, 104}

Though there is an increasing body of evidence that IB formation reflects a beneficial cellular homeostatic response to the burden of aggregation-prone protein,^{119, 121, 125, 139, 159} understanding how IBs might be protective has proven difficult. We found that a longitudinal single-cell approach allowed us to monitor differences within a population of cells that develop asynchronously and in a time-dependent fashion. In this study we find that improving UPS function may contribute to the benefits of IB formation, but other mechanisms of protection, such as increasing autophagic efficiency or preventing toxic protein-protein interactions, are possible as well.

Materials and Methods

Plasmids

The pGW1-GFP, pGW1-httQ72-eGFP, pGW1-mRFP mammalian expression plasmids have been described previously (Chapter 2).¹²⁵ mRFP1 was subcloned from pRSETB-mRFP1 (Dr. R. Tsien, UCSD, San Diego, CA) into pcDNA3.1(+) using BamHI/EcoRI. pGW1-mRFP^u (mRFP^u) was generated by subcloning mRFP1 from pcDNA3.1(+) into pEGFP-CL1 (Dr. R. Kopito, Stanford University, Stanford, CA) using NheI/EcoRI, removing the stop codon by swapping in annealed oligonucleotides (5'CCGGCGCCTATG3' and 5'AATTCATAGGCG3') into SgrAI/EcoRI digested vector and restoring frame with a AccI digest, Klenow reaction and blunt end ligation. mRFP1-CL1 was then excised using BamHI and inserted in the BglII site of pGW1Nhe. pGW1-GFP^u (GFP^u) was constructed by excising EGFP-CL1 from pEGFP-CL1 using NheI/BamHI and inserting in the NheI/BglII sites of pGW1Nhe (performed by V.

Rao). pGW1-Venus-CL1 (Venus^u) was generated by subcloning Venus from pCS2-Venus (Dr. A. Miyawaki, Brain Science Institute, RIKEN, Japan) into pcDNA3.1(+) using BamHI/EcoRI. The stop codon from Venus was removed and replaced by the sequence AGATCTCG. The CL1 sequence⁹⁶ was introduced into the EcoRI site at the 3' end of Venus and a linker from the pEGFP-C1 (Clontech, Mountain View, CA) MCS from the 3' end of EGFP to KpnI was inserted into the BsrGI site along with destroying the downstream BsrGI site. Venus-CL1 was then subcloned from pcDNA3.1(+) into pGW1-httQ25GFP, using KpnI/XbaI, replacing httQ25GFP. pCS2-Ub^{G76V}-Venus (Ub^{G76V}-Venus) was generated by PCR of Ub^{G76V} from Ub^{G76V}-GFP (Dr. N Dantuma, Karolinska Institutet, Stockholm, Sweden) using primers with flanking BamHI sites (5'AAAGCGGGATCCACCATGCAGATCTTCGTGAAGAC3' and 5'AAAGCGGGATCCCACCACACCTCTGAGACGGAG3'), digestion with BamHI and ligation into the BamHI site in pCS2-Venus.

Cell culture

Primary cultures of rat striatal neurons were prepared from embryos following 16-18 days of gestation as described previously (Chapter 2).^{121, 128} Briefly, striata were dissected in ice-cold DM/KY: dissociation medium (81.8mM Na₂SO₄, 30mM K₂SO₄, 15.2mM MgCl₂, 0.25mM CaCl₂, 1mM HEPES pH 7.4, 20mM glucose, and 0.001% phenol red) supplemented with 1mM Kynurenic acid (Sigma-Aldrich, St. Louis, MO). 10U/ml papain (Worthington Biochemical, Lakewood, NJ) was preincubated with 0.42mg/ml L-cysteine (Sigma-Aldrich, St. Louis, MO) in DM/KY in a 37°C water bath for 20-30 minutes. The tissue was then treated with the activated papain in two serial incubations of 15 minutes each at 37°C. The papain was removed by three washes of five minutes each at 37°C with 10mg/ml Trypsin Inhibitor (Sigma-Aldrich, St. Louis, MO) in DM/KY. The tissue was triturated to single cells in Optimem (Invitrogen, Carlsbad, CA) supplemented

with 20mM glucose. Cells were counted with Trypan blue, and plated at 5.8×10^5 cells per well in 24-well tissue culture plates coated with HMW Poly-D-Lysine and Laminin (BD Biosciences, San Jose, CA). Two hours later, media on the cells was replaced with 1 ml of modified neuronal culture medium (NCM), a basal medium of Eagle (Invitrogen, Carlsbad, CA) based growth medium containing serum (formulation available at <http://www.gladstone.ucsf.edu/gladstone/files/finkbeiner/Protocols/cprotocol.pdf>). Cells were fed every five-seven days by washing three times in basal medium of Eagle and replacement with equal measures of conditioned and fresh neuronal culture medium.

Transfection and pharmacology

Primary cultures were transfected five to seven days in vitro with combinations of pGW1-GFP^u and pGW1-mRFP, pGW1-mRFP^u and pGW1-GFP, pGW1-Venus^u or pCS2-Ub^{G76V}-Venus and pGW1-CFP, and pGW1-httQ72-eGFP, pGW1-mRFP^u and pGW1-BFP in a 1:1 or 1:1:1 molar ratio with 2-4 μ g total plasmid DNA per well. Primary neurons were washed three times in DMEM supplemented with 10mM Kynurenic acid (DMEM/KY) and incubated at 37°C/9.5% CO₂ for 30 minutes prior to transfection. Calcium chloride and DNA solutions were added dropwise to 2xHBS. Calcium phosphate precipitate was allowed to develop in the dark for 10-15 minutes and then added to the cells dropwise. Precipitate on the cells was allowed to develop between 15-30 minutes depending on the rate at which precipitate formed. Cells were treated with an osmotic shock solution (2% DMSO (Fisher Scientific, Fairlawn, NJ), 10% DMEM/KY in hepes buffered saline) for 1-2 minutes, washed twice with DMEM/KY, once with basal medium of Eagle, and the media was replaced with 1 ml of a 1:1 combination of conditioned and fresh NCM. MG132 (Sigma-Aldrich, St. Louis, MO), epoxomicin (Boston Biochem, Cambridge, MA), and Bafilomycin A1 (Sigma-Aldrich, St. Louis, MO) were added in 1 mL conditioned NCM per well 12-60 hours after transfection.

Live-cell imaging and analysis

The imaging was performed with a Nikon TE300 inverted microscope mounted on a vibration isolation table (Technical Manufacturing, Peabody, MA) using a long working-distance Nikon 20X (NA 0.45) objective. Images were detected and digitized using a Hamamatsu Orca II camera with a 12-bit/14-bit digital cooled charge-coupled device detector (Hamamatsu Photonics, Bridgewater, NJ). Stage movements and focusing were performed using a Proscan II stage controller (Prior Scientific, Rockland MA). Samples were illuminated with a 175W Xenon Lambda LS illuminator (Sutter Instruments, Novato, CA) with liquid light guide and fluorescence excitation and emission filters were placed into the light path using a computer-controlled Lambda 10-2 controller and two ten-position filter wheels (Sutter Instruments, Novato, CA). BFP, GFP and RFP images were captured using an 86014 beamsplitter and 350/50x;465/30m, 480/40x;517/30m and 580/20x;630/60m fluorescence filters (Chroma Corp, Rockingham, VT) respectively. CFP, Venus, and RFP images were captured using a 86006 beamsplitter and 420/35x;470/30m, 500/20x;535/30m, and 580/20x;630/60m fluorescence filters (Chroma Corp, Rockingham, VT). Algorithms for plate registration, stage movements, filter movements, focusing and acquisition were generated with Metamorph imaging software (MDS, Inc, Mississauga, Ontario, Canada). Thirteen images per fluorescence channel were captured per well and analyzed manually using Metamorph software. Survival analysis was performed with the Statview software package (SAS Institute, Cary, NC) and other statistical analysis was performed with Prism (Graphpad Software, San Diego, CA). The significance of differences in Kaplan-Meier survival curves were determined with the log-rank test.

Chapter 4: Concluding remarks

Understanding cause-effect relationships underlying disease

Elucidating the molecular mechanisms that govern the initiation and progression of pathological processes is central to understanding disease. Primary initiating events may trigger molecular changes related to disease in the same or neighboring cells.

Understanding disease relies on distinguishing between the roles of these changes in pathogenesis. Is a particular cellular phenomenon an intermediary in pathogenesis or a protective response that prolongs survival? To develop effective targeted molecular therapeutics, one must define the pathogenic role of a cellular phenomenon and determine its importance in disease progression.

The particular challenge of the nervous system

Neurodegenerative disease presents additional complexity. Although a toxic protein may be expressed widely among many tissues and cell types, gradual and asynchronous cell death often occurs only in specific neuronal subpopulations. Before cell death occurs, an overlapping but distinct subset of cells frequently demonstrates a common pathological correlate: deposited insoluble mutant protein. Standard approaches of cell population-based biochemistry and conventional time-lapse microscopy have had limited success in unraveling the cause-effect relationships that underlie cellular pathogenesis, including those of HD pathogenesis. Population-based approaches have been confounded by cell-type dependent variation in physiological responses to stimuli. Furthermore, following the fate of neurons with high temporal resolution has been difficult because of the stochastic death of neurons, which reduces population size and limits the ability of biochemical assays to detect change. Although conventional time-lapse microscopy has been useful for observing successive changes in single cells, it has

been limited by labor-intensive and user-biased data acquisition and by an inability to quantitatively assess the contribution of cellular changes to particular outcomes.

A new approach

We overcame many of these limitations by creating a novel synthesis of single-cell time-lapse microscopy, robotics, biophysics, and biostatistics. The integration of robotics and biostatistics has yielded significant advances in genomics and proteomics and this combination results in synergy when applied to cell biology as well. We assembled and validated a robotic imaging platform and integrated biophysical and biostatistical techniques with our platform. As a result, we could use survival analysis to quantify the magnitude and relative significance of multiple parameters on cellular outcome. Survival analysis is a powerful suite of statistical techniques that has been widely applied in engineering and clinical medicine to determine how factors or interventions affect the likelihood of a subsequent outcome. By using a longitudinal single-cell approach, we applied survival analysis to identify predictive factors for toxicity and the mechanisms underlying them.

Summary of findings

The work in this dissertation examined the relationship between two particular relationships that underly the pathogenesis of HD. When we began our investigation, the role of IBs in the progression of disease was unclear. In Chapter 2, we found that neurons that formed IBs survived longer than those that did not. Species of diffuse huntingtin that precede IB formation are likely to be the major mediators of toxicity. UPS dysfunction caused by both diffuse mutant htt and mutant htt IBs had been proposed as a potential mechanism for mutant htt toxicity. In Chapter 3, we examined UPS impairment accompanying cellular pathogenesis. We found that UPS impairment is toxic to neurons.

High levels of UPS impairment precede IB formation and lower levels follow. These are the first findings to unambiguously demonstrate that IB formation is beneficial to cells and that improving UPS function is one mechanism by which they may be protective.

Parallels in other neurodegenerative diseases

Examining other polyQ diseases by single-cell longitudinal analysis will help to determine whether the findings we have described are unique to HD. One hypothesis for the cause of toxicity from the polyQ protein ataxin 1 is that the major effect of polyQ expansion is to increase levels of protein. This hypothesis, which has support from experiments in transgenic *Drosophila* ataxin-1 models, predicts that overexpression of wild-type ataxin 1 would be sufficient to cause disease. Transient transfection of ataxin 1 in primary cortical cultures demonstrates that expression of either wild-type or mutant ataxin 1 is toxic (Fig 4.1). This finding, which bears further investigation, does not eliminate the possibility that ataxin 1 IBs may be protective through a similar mechanism to what we have described for mutant htt—by sequestering mutant protein and facilitating mutant protein degradation.

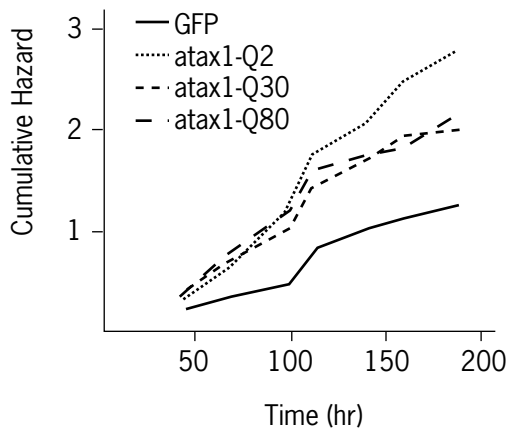


Figure 4.1. Ataxin-1 demonstrates polyQ-independent toxicity in primary cortical neurons. E17 cortical neurons were transfected 7 DIV with 1 μ g of either GW1-GFP, or pEGFP-ataxin1 with 2, 30, or 80 glutamines (Q2, Q30, Q80) and 1 μ g of pcDNA3.1(+)-mRFP. Over the following 7 days, all ataxin 1 constructs imparted a higher risk of death than GFP alone ($p < 0.01$), but there was no difference in hazard between Q2, Q30, and Q80.

Using a longitudinal approach to investigate neurodegenerative diseases caused by mutations in proteins without glutamine stretches may also be fruitful. Mutant SOD1 forms aggregates and causes degeneration of the spinal cord and brainstem in amyotrophic lateral sclerosis. We found that mutant SOD1 is toxic compared to wild-type SOD1 in primary cortical neurons (Fig 4.2). Examining this system more closely for IB formation and the relationship between protein levels and toxicity may help to determine if our findings are specific to polyQ disease.

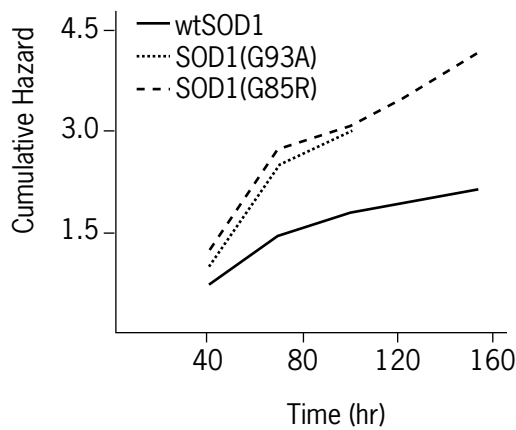


Figure 4.2. Mutants of SOD1 that cause ALS are toxic to primary striatal neurons. E17 striatal neurons were transfected with 1.5 μ g pCMV-SOD1wt-EGFP, SOD1(G85R)-EGFP or SOD1(G93A)-EGFP and 1.5 μ g pcDNA3.1(+)-mRFP. Over the following 6 days, both SOD1 mutants imparted a significantly higher risk of death than wild-type ($p < 0.005$).

The toxic species

Our results support a model for HD pathogenesis that centers on the diffuse species of mutant htt. The accumulation of mutant htt preceding IB formation may generate many htt species within the cell, including monomers and oligomers.¹⁶⁰ The relationships between these species and toxicity has not yet been determined. Because these species are likely in equilibrium within individual cells and because the aggregation process is asynchronous from cell to cell, population-based analysis will lack both sensitivity and specificity in addressing this relationship. An approach to monitor protein-

protein association in live cells as the disease progresses will be powerful in addressing the relationship between htt aggregation and toxicity.

Diffuse species of mutant htt are likely present throughout the lifetime of both the cell and the individual. A low probability nucleation event may explain the time-dependence of disease onset, but many of our experiments indicate that polyQ expansion in mutant htt introduces a constant, elevated risk of cellular death. One explanation for this finding could be that neurons die because they have been sensitized to stochastic perturbations in cellular homeostasis. Testing this hypothesis by reducing the “noise” in our culture system may be helpful. Noise may be caused by environmental stressors such as exposure to oxidative damage, which may be reduced by use of a low oxygen growth environment that may better mimic the extracellular conditions of the brain.

Mechanisms of toxicity

The mechanism by which diffuse species mediate toxicity remains unresolved. A direct effect by a specific protein-protein interaction with mutant htt remains a possibility. The relative contributions of more general mechanisms of toxicity such as an impairment of global UPS function¹⁴⁶ or autophagy remain hard to assess. The single-cell longitudinal system is an attractive approach to determine the relative contributions of multiple factors to an outcome. By using UPS and autophagy reporters in parallel and monitoring their relationship to mutant htt and neuronal survival, we may gain additional insight into the coordinate regulation of the two systems and how they contribute to HD pathogenesis.

The need for therapies

Translating our findings about mechanisms of toxicity to the development of treatments for patients remains a priority. The need for HD therapies is underscored by the lack of therapy to even slow progression of the disease.¹¹⁰ Our findings suggest that a

shift in focus might be beneficial in cell-based assays for drug screening. While a number of screens have looked for inhibitors of htt aggregation or IB formation,¹⁶¹ our results here suggest that identification of molecules that lower intracellular mutant htt levels or promote IB formation may be helpful. Some drugs that reduce IB formation will be protective but are likely to be beneficial by reducing levels of htt generally.

Our automated imaging platform and use of single-cell imaging represents a significant improvement in the sensitivity and specificity of systems for cell-based target identification, validation, and molecular refinement. The ability to distinguish between an effect in a subset of cells and a partial effect globally will help to understand some of the variability seen in cell culture. The identification of genes that modify htt toxicity in mammalian neurons is the first step in identifying targets for new classes of drugs to treat HD.

References

1. Sloane, P.D., et al., The public health impact of Alzheimer's disease, 2000-2050: potential implication of treatment advances. *Annu Rev Public Health*, 2002. 23: p. 213-31.
2. Brookmeyer, R., S. Gray, and C. Kawas, Projections of Alzheimer's disease in the United States and the public health impact of delaying disease onset. *Am J Public Health*, 1998. 88(9): p. 1337-42.
3. Walker, F.O., Huntington's disease. *Lancet*, 2007. 369(9557): p. 218-28.
4. Foroud, T., et al., Differences in duration of Huntington's disease based on age at onset. *J Neurol Neurosurg Psychiatry*, 1999. 66(1): p. 52-6.
5. Mahant, N., et al., Huntington's disease: clinical correlates of disability and progression. *Neurology*, 2003. 61(8): p. 1085-92.
6. Paulsen, J.S., et al., Critical periods of suicide risk in Huntington's disease. *Am J Psychiatry*, 2005. 162(4): p. 725-31.
7. Johnson, S.A., et al., Beyond disgust: impaired recognition of negative emotions prior to diagnosis in Huntington's disease. *Brain*, 2007. 130(Pt 7): p. 1732-44.
8. Gray, J.M., et al., Impaired recognition of disgust in Huntington's disease gene carriers. *Brain*, 1997. 120 (Pt 11): p. 2029-38.
9. Sprengelmeyer, R., et al., Disgust in pre-clinical Huntington's disease: a longitudinal study. *Neuropsychologia*, 2006. 44(4): p. 518-33.
10. Solomon, A.C., et al., Verbal episodic memory declines prior to diagnosis in Huntington's disease. *Neuropsychologia*, 2007. 45(8): p. 1767-76.
11. Snowden, J.S., et al., Awareness of involuntary movements in Huntington disease. *Arch Neurol*, 1998. 55(6): p. 801-5.

12. Feigin, A., et al., Functional decline in Huntington's disease. *Mov Disord*, 1995. 10(2): p. 211-4.
13. Donald, R.G. and D.S. Roos, Stable molecular transformation of *Toxoplasma gondii*: a selectable dihydrofolate reductase-thymidylate synthase marker based on drug-resistance mutations in malaria. *Proc Natl Acad Sci U S A*, 1993. 90(24): p. 11703-7.
14. Ashizawa, T., et al., CAG repeat size and clinical presentation in Huntington's disease. *Neurology*, 1994. 44(6): p. 1137-43.
15. Squitieri, F., M. Cannella, and M. Simonelli, CAG mutation effect on rate of progression in Huntington's disease. *Neurol Sci*, 2002. 23 Suppl 2: p. S107-8.
16. Gusella, J.F., et al., A polymorphic DNA marker genetically linked to Huntington's disease. *Nature*, 1983. 306(5940): p. 234-8.
17. A novel gene containing a trinucleotide repeat that is expanded and unstable on Huntington's disease chromosomes. The Huntington's Disease Collaborative Research Group. *Cell*, 1993. 72(6): p. 971-83.
18. Fu, Y.H., et al., Variation of the CGG repeat at the fragile X site results in genetic instability: resolution of the Sherman paradox. *Cell*, 1991. 67(6): p. 1047-58.
19. Pieretti, M., et al., Absence of expression of the FMR-1 gene in fragile X syndrome. *Cell*, 1991. 66(4): p. 817-22.
20. Verkerk, A.J., et al., Identification of a gene (FMR-1) containing a CGG repeat coincident with a breakpoint cluster region exhibiting length variation in fragile X syndrome. *Cell*, 1991. 65(5): p. 905-14.
21. Aslanidis, C., et al., Cloning of the essential myotonic dystrophy region and mapping of the putative defect. *Nature*, 1992. 355(6360): p. 548-51.
22. Buxton, J., et al., Detection of an unstable fragment of DNA specific to individuals with myotonic dystrophy. *Nature*, 1992. 355(6360): p. 547-8.

23. La Spada, A.R., et al., Androgen receptor gene mutations in X-linked spinal and bulbar muscular atrophy. *Nature*, 1991. 352(6330): p. 77-9.
24. Nagafuchi, S., et al., Structure and expression of the gene responsible for the triplet repeat disorder, dentatorubral and pallidolusian atrophy (DRPLA). *Nat Genet*, 1994. 8(2): p. 177-82.
25. Koide, R., et al., Unstable expansion of CAG repeat in hereditary dentatorubral-pallidolusian atrophy (DRPLA). *Nat Genet*, 1994. 6(1): p. 9-13.
26. Nagafuchi, S., et al., Dentatorubral and pallidolusian atrophy expansion of an unstable CAG trinucleotide on chromosome 12p. *Nat Genet*, 1994. 6(1): p. 14-8.
27. Zoghbi, H.Y. and H.T. Orr, Glutamine repeats and neurodegeneration. *Annu Rev Neurosci*, 2000. 23: p. 217-47.
28. Duyao, M., et al., Trinucleotide repeat length instability and age of onset in Huntington's disease. *Nat Genet*, 1993. 4(4): p. 387-92.
29. Trottier, Y., V. Biancalana, and J.L. Mandel, Instability of CAG repeats in Huntington's disease: relation to parental transmission and age of onset. *J Med Genet*, 1994. 31(5): p. 377-82.
30. MacDonald, M.E., et al., Gametic but not somatic instability of CAG repeat length in Huntington's disease. *J Med Genet*, 1993. 30(12): p. 982-6.
31. Zuhlke, C., et al., Mitotic stability and meiotic variability of the (CAG)_n repeat in the Huntington disease gene. *Hum Mol Genet*, 1993. 2(12): p. 2063-7.
32. Telenius, H., et al., Somatic and gonadal mosaicism of the Huntington disease gene CAG repeat in brain and sperm. *Nat Genet*, 1994. 6(4): p. 409-14.
33. Lahiri, M., et al., Expanded CAG repeats activate the DNA damage checkpoint pathway. *Mol Cell*, 2004. 15(2): p. 287-93.
34. Kovtun, I.V., et al., OGG1 initiates age-dependent CAG trinucleotide expansion in somatic cells. *Nature*, 2007. 447(7143): p. 447-52.

35. Andrew, S.E., et al., The relationship between trinucleotide (CAG) repeat length and clinical features of Huntington's disease. *Nat Genet*, 1993. 4(4): p. 398-403.
36. Snell, R.G., et al., Relationship between trinucleotide repeat expansion and phenotypic variation in Huntington's disease. *Nat Genet*, 1993. 4(4): p. 393-7.
37. Langbehn, D.R., et al., A new model for prediction of the age of onset and penetrance for Huntington's disease based on CAG length. *Clin Genet*, 2004. 65(4): p. 267-77.
38. Graveland, G.A., R.S. Williams, and M. DiFiglia, Evidence for degenerative and regenerative changes in neostriatal spiny neurons in Huntington's disease. *Science*, 1985. 227(4688): p. 770-3.
39. Vonsattel, J.P., et al., Neuropathological classification of Huntington's disease. *J Neuropathol Exp Neurol*, 1985. 44(6): p. 559-77.
40. de la Monte, S.M., J.P. Vonsattel, and E.P. Richardson, Jr., Morphometric demonstration of atrophic changes in the cerebral cortex, white matter, and neostriatum in Huntington's disease. *J Neuropathol Exp Neurol*, 1988. 47(5): p. 516-25.
41. Sax, D.S., et al., Computed tomographic, neurologic, and neuropsychological correlates of Huntington's disease. *Int J Neurosci*, 1983. 18(1-2): p. 21-36.
42. Strong, T.V., et al., Widespread expression of the human and rat Huntington's disease gene in brain and nonneural tissues. *Nat Genet*, 1993. 5(3): p. 259-65.
43. Sharp, A.H., et al., Widespread expression of Huntington's disease gene (IT15) protein product. *Neuron*, 1995. 14(5): p. 1065-74.
44. Ferrante, R.J., et al., Heterogeneous topographic and cellular distribution of huntingtin expression in the normal human neostriatum. *J Neurosci*, 1997. 17(9): p. 3052-63.

45. Duyao, M.P., et al., Inactivation of the mouse Huntington's disease gene homolog Hdh. *Science*, 1995. 269(5222): p. 407-10.
46. Nasir, J., et al., Targeted disruption of the Huntington's disease gene results in embryonic lethality and behavioral and morphological changes in heterozygotes. *Cell*, 1995. 81(5): p. 811-23.
47. Bhide, P.G., et al., Expression of normal and mutant huntingtin in the developing brain. *J Neurosci*, 1996. 16(17): p. 5523-35.
48. Hodgson, J.G., et al., Human huntingtin derived from YAC transgenes compensates for loss of murine huntingtin by rescue of the embryonic lethal phenotype. *Hum Mol Genet*, 1996. 5(12): p. 1875-85.
49. Dragatsis, I., M.S. Levine, and S. Zeitlin, Inactivation of Hdh in the brain and testis results in progressive neurodegeneration and sterility in mice. *Nat Genet*, 2000. 26(3): p. 300-6.
50. Li, H., et al., Amino-terminal fragments of mutant huntingtin show selective accumulation in striatal neurons and synaptic toxicity. *Nat Genet*, 2000. 25(4): p. 385-9.
51. Li, H., et al., Abnormal association of mutant huntingtin with synaptic vesicles inhibits glutamate release. *Hum Mol Genet*, 2003. 12(16): p. 2021-30.
52. Gunawardena, S., et al., Disruption of axonal transport by loss of huntingtin or expression of pathogenic polyQ proteins in *Drosophila*. *Neuron*, 2003. 40(1): p. 25-40.
53. Szebenyi, G., et al., Neuropathogenic forms of huntingtin and androgen receptor inhibit fast axonal transport. *Neuron*, 2003. 40(1): p. 41-52.
54. Schaffar, G., et al., Cellular toxicity of polyglutamine expansion proteins: mechanism of transcription factor deactivation. *Mol Cell*, 2004. 15(1): p. 95-105.

55. Cepeda, C., et al., Transient and progressive electrophysiological alterations in the corticostriatal pathway in a mouse model of Huntington's disease. *J Neurosci*, 2003. 23(3): p. 961-9.
56. Laforet, G.A., et al., Changes in cortical and striatal neurons predict behavioral and electrophysiological abnormalities in a transgenic murine model of Huntington's disease. *J Neurosci*, 2001. 21(23): p. 9112-23.
57. Zeron, M.M., et al., Mutant huntingtin enhances excitotoxic cell death. *Mol Cell Neurosci*, 2001. 17(1): p. 41-53.
58. Zeron, M.M., et al., Increased sensitivity to N-methyl-D-aspartate receptor-mediated excitotoxicity in a mouse model of Huntington's disease. *Neuron*, 2002. 33(6): p. 849-60.
59. Mangiarini, L., et al., Exon 1 of the HD gene with an expanded CAG repeat is sufficient to cause a progressive neurological phenotype in transgenic mice. *Cell*, 1996. 87(3): p. 493-506.
60. Hodgson, J.G., et al., A YAC mouse model for Huntington's disease with full-length mutant huntingtin, cytoplasmic toxicity, and selective striatal neurodegeneration. *Neuron*, 1999. 23(1): p. 181-92.
61. Goldberg, Y.P., et al., Cleavage of huntingtin by apopain, a proapoptotic cysteine protease, is modulated by the polyglutamine tract. *Nat Genet*, 1996. 13(4): p. 442-9.
62. Wellington, C.L., et al., Caspase cleavage of gene products associated with triplet expansion disorders generates truncated fragments containing the polyglutamine tract. *J Biol Chem*, 1998. 273(15): p. 9158-67.
63. Wellington, C.L., et al., Inhibiting caspase cleavage of huntingtin reduces toxicity and aggregate formation in neuronal and nonneuronal cells. *J Biol Chem*, 2000. 275(26): p. 19831-8.

64. Kim, Y.J., et al., Caspase 3-cleaved N-terminal fragments of wild-type and mutant huntingtin are present in normal and Huntington's disease brains, associate with membranes, and undergo calpain-dependent proteolysis. *Proc Natl Acad Sci U S A*, 2001. 98(22): p. 12784-9.
65. Kim, M., et al., Mutant huntingtin expression in clonal striatal cells: dissociation of inclusion formation and neuronal survival by caspase inhibition. *J Neurosci*, 1999. 19(3): p. 964-73.
66. Hackam, A.S., et al., Huntingtin interacting protein 1 induces apoptosis via a novel caspase-dependent death effector domain. *J Biol Chem*, 2000. 275(52): p. 41299-308.
67. Li, S.H., et al., Intranuclear huntingtin increases the expression of caspase-1 and induces apoptosis. *Hum Mol Genet*, 2000. 9(19): p. 2859-67.
68. Lunkes, A., et al., Proteases acting on mutant huntingtin generate cleaved products that differentially build up cytoplasmic and nuclear inclusions. *Mol Cell*, 2002. 10(2): p. 259-69.
69. Graham, R.K., et al., Cleavage at the caspase-6 site is required for neuronal dysfunction and degeneration due to mutant huntingtin. *Cell*, 2006. 125(6): p. 1179-91.
70. DiFiglia, M., et al., Aggregation of huntingtin in neuronal intranuclear inclusions and dystrophic neurites in brain. *Science*, 1997. 277(5334): p. 1990-3.
71. Davies, S.W., et al., Formation of neuronal intranuclear inclusions underlies the neurological dysfunction in mice transgenic for the HD mutation. *Cell*, 1997. 90(3): p. 537-48.
72. Wanderer, J. and A.J. Morton, Differential morphology and composition of inclusions in the R6/2 mouse and PC12 cell models of Huntington's disease. *Histochem Cell Biol*, 2007. 127(5): p. 473-84.

73. Kazantsev, A., et al., Insoluble detergent-resistant aggregates form between pathological and nonpathological lengths of polyglutamine in mammalian cells. *Proc Natl Acad Sci U S A*, 1999. 96(20): p. 11404-9.
74. Boutell, J.M., et al., Aberrant interactions of transcriptional repressor proteins with the Huntington's disease gene product, huntingtin. *Hum Mol Genet*, 1999. 8(9): p. 1647-55.
75. Steffan, J.S., et al., The Huntington's disease protein interacts with p53 and CREB-binding protein and represses transcription. *Proc Natl Acad Sci U S A*, 2000. 97(12): p. 6763-8.
76. Holbert, S., et al., The Gln-Ala repeat transcriptional activator CA150 interacts with huntingtin: neuropathologic and genetic evidence for a role in Huntington's disease pathogenesis. *Proc Natl Acad Sci U S A*, 2001. 98(4): p. 1811-6.
77. Dunah, A.W., et al., Sp1 and TAFII130 transcriptional activity disrupted in early Huntington's disease. *Science*, 2002. 296(5576): p. 2238-43.
78. Suhr, S.T., et al., Identities of sequestered proteins in aggregates from cells with induced polyglutamine expression. *J Cell Biol*, 2001. 153(2): p. 283-94.
79. Obrietan, K. and K.R. Hoyt, CRE-mediated transcription is increased in Huntington's disease transgenic mice. *J Neurosci*, 2004. 24(4): p. 791-6.
80. Nucifora, F.C., Jr., et al., Interference by huntingtin and atrophin-1 with cbp-mediated transcription leading to cellular toxicity. *Science*, 2001. 291(5512): p. 2423-8.
81. Zuccato, C., et al., Loss of huntingtin-mediated BDNF gene transcription in Huntington's disease. *Science*, 2001. 293(5529): p. 493-8.
82. Zuccato, C., et al., Huntingtin interacts with REST/NRSF to modulate the transcription of NRSE-controlled neuronal genes. *Nat Genet*, 2003.

83. Iwata, A., et al., Increased susceptibility of cytoplasmic over nuclear polyglutamine aggregates to autophagic degradation. *Proc Natl Acad Sci U S A*, 2005. 102(37): p. 13135-40.
84. Frydman, J., FOLDING OF NEWLY TRANSLATED PROTEINS IN VIVO: The Role of Molecular Chaperones. *Annu Rev Biochem*, 2001. 70: p. 603-647.
85. Chai, Y., et al., Analysis of the role of heat shock protein (Hsp) molecular chaperones in polyglutamine disease. *J Neurosci*, 1999. 19(23): p. 10338-47.
86. Kazemi-Esfarjani, P. and S. Benzer, Genetic suppression of polyglutamine toxicity in *Drosophila*. *Science*, 2000. 287(5459): p. 1837-40.
87. Cummings, C.J., et al., Chaperone suppression of aggregation and altered subcellular proteasome localization imply protein misfolding in SCA1. *Nat Genet*, 1998. 19(2): p. 148-54.
88. Stenoien, D.L., et al., Polyglutamine-expanded androgen receptors form aggregates that sequester heat shock proteins, proteasome components and SRC-1, and are suppressed by the HDJ-2 chaperone. *Hum Mol Genet*, 1999. 8(5): p. 731-41.
89. Warrick, J.M., et al., Suppression of polyglutamine-mediated neurodegeneration in *Drosophila* by the molecular chaperone HSP70. *Nat Genet*, 1999. 23(4): p. 425-8.
90. Cummings, C.J., et al., Over-expression of inducible HSP70 chaperone suppresses neuropathology and improves motor function in SCA1 mice. *Hum Mol Genet*, 2001. 10(14): p. 1511-8.
91. Jana, N.R., et al., Polyglutamine length-dependent interaction of Hsp40 and Hsp70 family chaperones with truncated N-terminal huntingtin: their role in suppression of aggregation and cellular toxicity. *Hum Mol Genet*, 2000. 9(13): p. 2009-18.
92. Zhou, H., S.H. Li, and X.J. Li, Chaperone suppression of cellular toxicity of huntingtin is independent of polyglutamine aggregation. *J Biol Chem*, 2001. 276(51): p. 48417-24.

93. Hansson, O., et al., Overexpression of heat shock protein 70 in R6/2 Huntington's disease mice has only modest effects on disease progression. *Brain Res*, 2003. 970(1-2): p. 47-57.
94. Hochstrasser, M., Ubiquitin-dependent protein degradation. *Annu Rev Genet*, 1996. 30: p. 405-39.
95. Naujokat, C. and S. Hoffmann, Role and function of the 26S proteasome in proliferation and apoptosis. *Lab Invest*, 2002. 82(8): p. 965-80.
96. Bence, N.F., R.M. Sampat, and R.R. Kopito, Impairment of the ubiquitin-proteasome system by protein aggregation. *Science*, 2001. 292(5521): p. 1552-5.
97. Stenoien, D.L., M. Mielke, and M.A. Mancini, Intranuclear ataxin1 inclusions contain both fast- and slow-exchanging components. *Nat Cell Biol*, 2002. 4(10): p. 806-10.
98. Matsumoto, G., et al., Structural properties and neuronal toxicity of amyotrophic lateral sclerosis-associated Cu/Zn superoxide dismutase 1 aggregates. *J Cell Biol*, 2005. 171(1): p. 75-85.
99. Matsumoto, G., S. Kim, and R.I. Morimoto, Huntingtin and mutant SOD1 form aggregate structures with distinct molecular properties in human cells. *J Biol Chem*, 2006. 281(7): p. 4477-85.
100. Klionsky, D.J. and S.D. Emr, Autophagy as a regulated pathway of cellular degradation. *Science*, 2000. 290(5497): p. 1717-21.
101. Thumm, M., et al., Isolation of autophagocytosis mutants of *Saccharomyces cerevisiae*. *FEBS Lett*, 1994. 349(2): p. 275-80.
102. Cuervo, A.M., Autophagy in neurons: it is not all about food. *Trends Mol Med*, 2006. 12(10): p. 461-4.
103. Hara, T., et al., Suppression of basal autophagy in neural cells causes neurodegenerative disease in mice. *Nature*, 2006. 441(7095): p. 885-9.

104. Komatsu, M., et al., Loss of autophagy in the central nervous system causes neurodegeneration in mice. *Nature*, 2006. 441(7095): p. 880-4.
105. Ravikumar, B., R. Duden, and D.C. Rubinsztein, Aggregate-prone proteins with polyglutamine and polyalanine expansions are degraded by autophagy. *Hum Mol Genet*, 2002. 11(9): p. 1107-17.
106. Ravikumar, B., et al., Inhibition of mTOR induces autophagy and reduces toxicity of polyglutamine expansions in fly and mouse models of Huntington disease. *Nat Genet*, 2004. 36(6): p. 585-95.
107. Kawaguchi, Y., et al., The deacetylase HDAC6 regulates aggresome formation and cell viability in response to misfolded protein stress. *Cell*, 2003. 115(6): p. 727-38.
108. Iwata, A., et al., HDAC6 and microtubules are required for autophagic degradation of aggregated huntingtin. *J Biol Chem*, 2005. 280(48): p. 40282-92.
109. Pandey, U.B., et al., HDAC6 rescues neurodegeneration and provides an essential link between autophagy and the UPS. *Nature*, 2007. 447(7146): p. 859-63.
110. Hersch, S.M., Huntington's disease: prospects for neuroprotective therapy 10 years after the discovery of the causative genetic mutation. *Curr Opin Neurol*, 2003. 16(4): p. 501-6.
111. Gusella, J.F. and M.E. MacDonald, Molecular genetics: unmasking polyglutamine triggers in neurodegenerative disease. *Nat Rev Neurosci*, 2000. 1(2): p. 109-15.
112. Sittler, A., et al., Geldanamycin activates a heat shock response and inhibits huntingtin aggregation in a cell culture model of Huntington's disease. *Hum Mol Genet*, 2001. 10(12): p. 1307-15.
113. Khoshnan, A., J. Ko, and P.H. Patterson, Effects of intracellular expression of anti-huntingtin antibodies of various specificities on mutant huntingtin aggregation and toxicity. *Proc Natl Acad Sci U S A*, 2002. 99(2): p. 1002-7.

114. Baxter, M.G. and E.A. Murray, The amygdala and reward. *Nat Rev Neurosci*, 2002. 3(7): p. 563-73.
115. Carmichael, J., et al., Bacterial and yeast chaperones reduce both aggregate formation and cell death in mammalian cell models of Huntington's disease. *Proc Natl Acad Sci U S A*, 2000. 97(17): p. 9701-5.
116. Humbert, S., et al., The IGF-1/Akt pathway is neuroprotective in Huntington's disease and involves Huntingtin phosphorylation by Akt. *Dev Cell*, 2002. 2(6): p. 831-7.
117. Verhoef, L.G., et al., Aggregate formation inhibits proteasomal degradation of polyglutamine proteins. *Hum Mol Genet*, 2002. 11(22): p. 2689-700.
118. Tsai, Y.C., et al., Parkin facilitates the elimination of expanded polyglutamine proteins and leads to preservation of proteasome function. *J Biol Chem*, 2003. 278(24): p. 22044-55.
119. Klement, I.A., et al., Ataxin-1 nuclear localization and aggregation: role in polyglutamine-induced disease in SCA1 transgenic mice. *Cell*, 1998. 95(1): p. 41-53.
120. Leavitt, B.R., C.L. Wellington, and M.R. Hayden, Recent insights into the molecular pathogenesis of Huntington disease. *Semin Neurol*, 1999. 19(4): p. 385-95.
121. Saudou, F., et al., Huntingtin acts in the nucleus to induce apoptosis but death does not correlate with the formation of intranuclear inclusions. *Cell*, 1998. 95(1): p. 55-66.
122. Arrasate, M. and S. Finkbeiner, Automated microscope system for determining factors that predict neuronal fate. *Proc Natl Acad Sci U S A*, 2005. 102(10): p. 3840-5.
123. Tsien, R.Y., The green fluorescent protein. *Annu Rev Biochem*, 1998. 67: p. 509-44.

124. Campbell, R.E., et al., A monomeric red fluorescent protein. *Proc Natl Acad Sci U S A*, 2002. 99(12): p. 7877-82.
125. Arrasate, M., et al., Inclusion body formation reduces levels of mutant huntingtin and the risk of neuronal death. *Nature*, 2004. 431(7010): p. 805-10.
126. Fortun, J., et al., Impaired proteasome activity and accumulation of ubiquitinated substrates in a hereditary neuropathy model. *J Neurochem*, 2005. 92(6): p. 1531-41.
127. Bennett, E.J., et al., Global impairment of the ubiquitin-proteasome system by nuclear or cytoplasmic protein aggregates precedes inclusion body formation. *Mol Cell*, 2005. 17(3): p. 351-65.
128. Finkbeiner, S., et al., CREB: a major mediator of neuronal neurotrophin responses. *Neuron*, 1997. 19(5): p. 1031-47.
129. Hershko, A. and A. Ciechanover, The ubiquitin system. *Annu Rev Biochem*, 1998. 67: p. 425-79.
130. Sherman, M.Y. and A.L. Goldberg, Cellular defenses against unfolded proteins: a cell biologist thinks about neurodegenerative diseases. *Neuron*, 2001. 29(1): p. 15-32.
131. Keller, J.N., J. Gee, and Q. Ding, The proteasome in brain aging. *Ageing Res Rev*, 2002. 1(2): p. 279-93.
132. Ding, Q. and J.N. Keller, Proteasomes and proteasome inhibition in the central nervous system. *Free Radic Biol Med*, 2001. 31(5): p. 574-84.
133. Rusmini, P., et al., Aggregation and proteasome: the case of elongated polyglutamine aggregation in spinal and bulbar muscular atrophy. *Neurobiol Aging*, 2007. 28(7): p. 1099-111.

134. Waelter, S., et al., Accumulation of mutant huntingtin fragments in aggresome-like inclusion bodies as a result of insufficient protein degradation. *Mol Biol Cell*, 2001. 12(5): p. 1393-407.
135. Hazeki, N., et al., Ultrastructure of nuclear aggregates formed by expressing an expanded polyglutamine. *Biochem Biophys Res Commun*, 2002. 294(2): p. 429-40.
136. Chai, Y., et al., Live-cell imaging reveals divergent intracellular dynamics of polyglutamine disease proteins and supports a sequestration model of pathogenesis. *Proc Natl Acad Sci U S A*, 2002. 99(14): p. 9310-5.
137. Ding, Q., et al., Polyglutamine expansion, protein aggregation, proteasome activity, and neural survival. *J Biol Chem*, 2002. 277(16): p. 13935-42.
138. Holmberg, C.I., et al., Inefficient degradation of truncated polyglutamine proteins by the proteasome. *EMBO J*, 2004. 23(21): p. 4307-18.
139. Taylor, J.P., et al., Aggresomes protect cells by enhancing the degradation of toxic polyglutamine-containing protein. *Hum Mol Genet*, 2003. 12(7): p. 749-57.
140. Gilon, T., O. Chomsky, and R.G. Kulka, Degradation signals for ubiquitin system proteolysis in *Saccharomyces cerevisiae*. *Embo J*, 1998. 17(10): p. 2759-66.
141. Dantuma, N.P., et al., Short-lived green fluorescent proteins for quantifying ubiquitin/proteasome-dependent proteolysis in living cells. *Nat Biotechnol*, 2000. 18(5): p. 538-43.
142. Nagai, T., et al., A variant of yellow fluorescent protein with fast and efficient maturation for cell-biological applications. *Nat Biotechnol*, 2002. 20(1): p. 87-90.
143. Yoshimori, T., et al., Bafilomycin A1, a specific inhibitor of vacuolar-type H(+)-ATPase, inhibits acidification and protein degradation in lysosomes of cultured cells. *J Biol Chem*, 1991. 266(26): p. 17707-12.

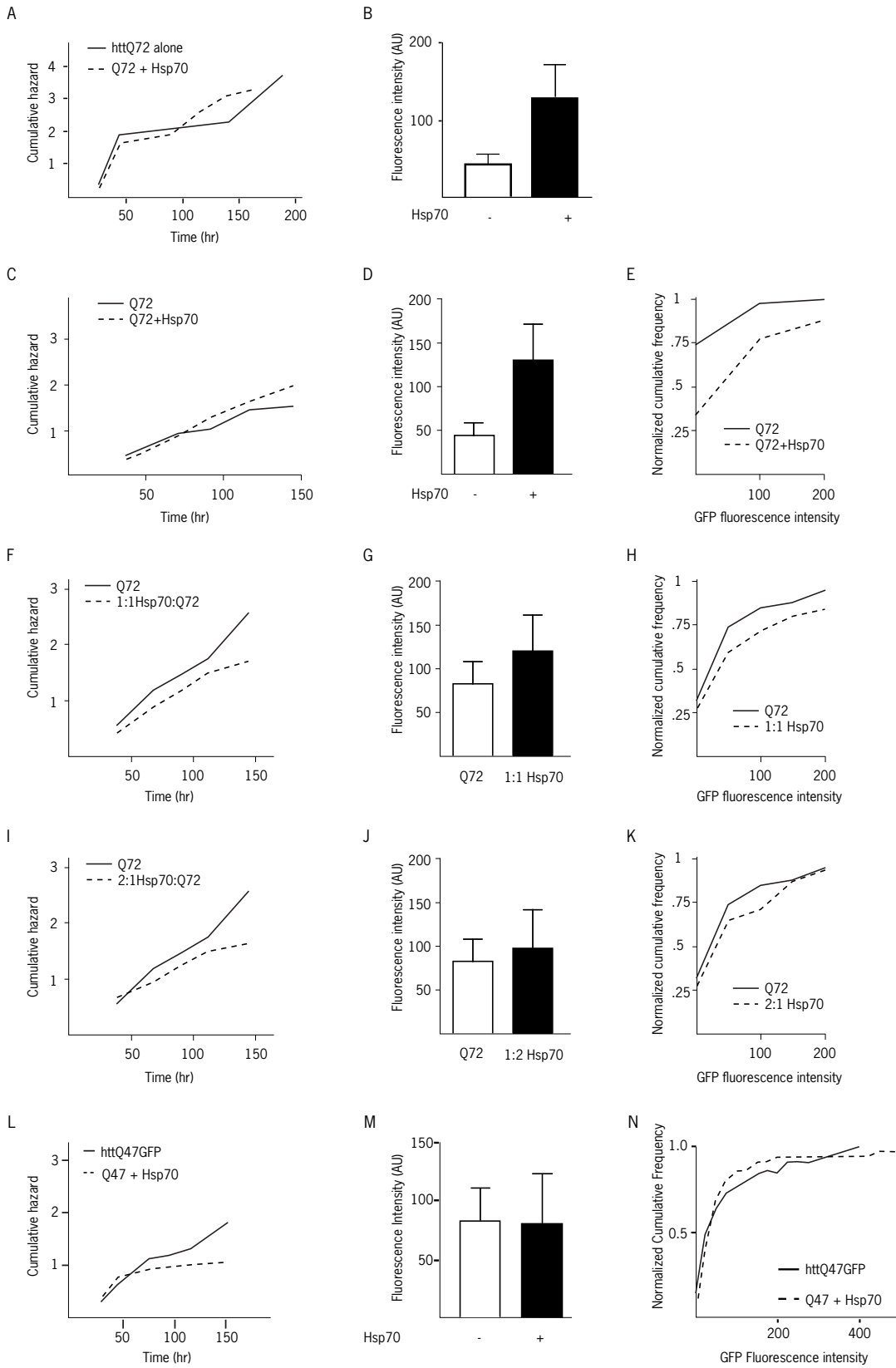
144. Yamamoto, A., et al., Bafilomycin A1 prevents maturation of autophagic vacuoles by inhibiting fusion between autophagosomes and lysosomes in rat hepatoma cell line, H-4-II-E cells. *Cell Struct Funct*, 1998. 23(1): p. 33-42.
145. Mizushima, N. and T. Yoshimori, How to Interpret LC3 Immunoblotting. *Autophagy*, 2007. 3(6).
146. Bennett, E.J., et al., Global changes to the ubiquitin system in Huntington's disease. *Nature*, 2007. 448(7154): p. 704-8.
147. Petersen, A., et al., Expanded CAG repeats in exon 1 of the Huntington's disease gene stimulate dopamine-mediated striatal neuron autophagy and degeneration. *Hum Mol Genet*, 2001. 10(12): p. 1243-54.
148. Qin, Z.H., et al., Autophagy regulates the processing of amino terminal huntingtin fragments. *Hum Mol Genet*, 2003. 12(24): p. 3231-44.
149. Webb, J.L., et al., Alpha-Synuclein is degraded by both autophagy and the proteasome. *J Biol Chem*, 2003. 278(27): p. 25009-13.
150. Berger, Z., et al., Rapamycin alleviates toxicity of different aggregate-prone proteins. *Hum Mol Genet*, 2006. 15(3): p. 433-42.
151. Ravikumar, B., et al., Rapamycin pre-treatment protects against apoptosis. *Hum Mol Genet*, 2006. 15(7): p. 1209-16.
152. Rubinsztein, D.C., The roles of intracellular protein-degradation pathways in neurodegeneration. *Nature*, 2006. 443(7113): p. 780-6.
153. Venkatraman, P., et al., Eukaryotic proteasomes cannot digest polyglutamine sequences and release them during degradation of polyglutamine-containing proteins. *Mol Cell*, 2004. 14(1): p. 95-104.
154. Mizushima, N., Collaboration of proteolytic systems. *Autophagy*, 2007. 3(3): p. 179-80.

155. Almeida, C.G., R.H. Takahashi, and G.K. Gouras, Beta-amyloid accumulation impairs multivesicular body sorting by inhibiting the ubiquitin-proteasome system. *J Neurosci*, 2006. 26(16): p. 4277-88.
156. Harada, M., et al., Proteasome inhibition induces inclusion bodies associated with intermediate filaments and fragmentation of the Golgi apparatus. *Exp Cell Res*, 2003. 288(1): p. 60-9.
157. Massey, A.C., C. Zhang, and A.M. Cuervo, Chaperone-mediated autophagy in aging and disease. *Curr Top Dev Biol*, 2006. 73: p. 205-35.
158. Mizushima, N., et al., In vivo analysis of autophagy in response to nutrient starvation using transgenic mice expressing a fluorescent autophagosome marker. *Mol Biol Cell*, 2004. 15(3): p. 1101-11.
159. Cummings, C.J., et al., Mutation of the E6-AP ubiquitin ligase reduces nuclear inclusion frequency while accelerating polyglutamine-induced pathology in SCA1 mice. *Neuron*, 1999. 24(4): p. 879-92.
160. Iuchi, S., et al., Oligomeric and polymeric aggregates formed by proteins containing expanded polyglutamine. *Proc Natl Acad Sci U S A*, 2003. 100(5): p. 2409-14.
161. Pollitt, S.K., et al., A rapid cellular FRET assay of polyglutamine aggregation identifies a novel inhibitor. *Neuron*, 2003. 40(4): p. 685-94.

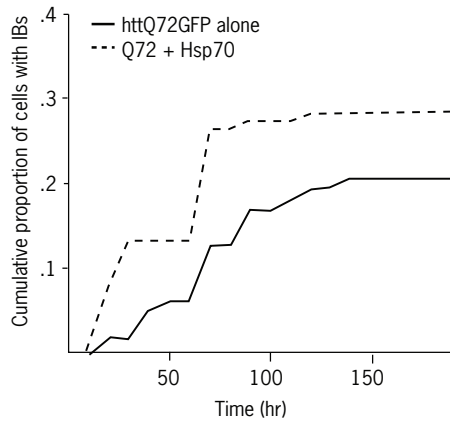
Appendix 1:

Trans-acting factors and the cellular pathogenesis of HD

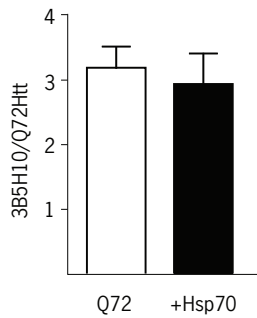
Chaperones



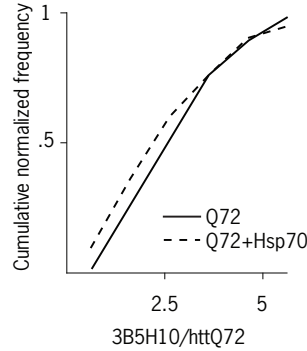
O



P



Q



R

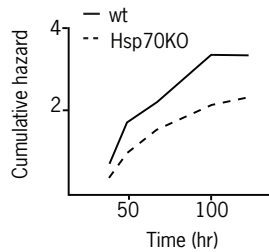


Figure A.1. Hsp70 either increases survival or htt levels in cells with mutant htt. E17-19 striatal cells were transfected 5-7 DIV with 1 μ g each of pGW1-httQ72GFP or pGW1-httQ47GFP, Hsp70 (Finkbeiner plasmid library location: F14) or pcDNA3.1(+) and pcDNA3.1(+)-mRFP except for one experiment (I-K) where 2 μ g of Hsp70 were used. Some experiments (A-E) demonstrated that Hsp70 increased htt levels between 18-24 hours following transfection (B,D,E) but resulted in a similar risk of death as the empty pcDNA3.1(+) vector (A,C). Other experiments in which the addition of Hsp70 did not change htt levels significantly (F-N) showed that Hsp70 had a small pro-survival benefit (F,I,L). In those experiments with a significant increase in htt levels, IB formation was faster and occurred in a larger proportion of cells (O). In parallel experiments, Hsp70 had no effect on the relative amount of 3B5H10 epitope per cell either in mean 3B5H10/htt ratio (P) or in single-cell distributions (Q). Curiously, mouse cells without Hsp70 survived better than wild-type cells when transfected with httQ72GFP (R).

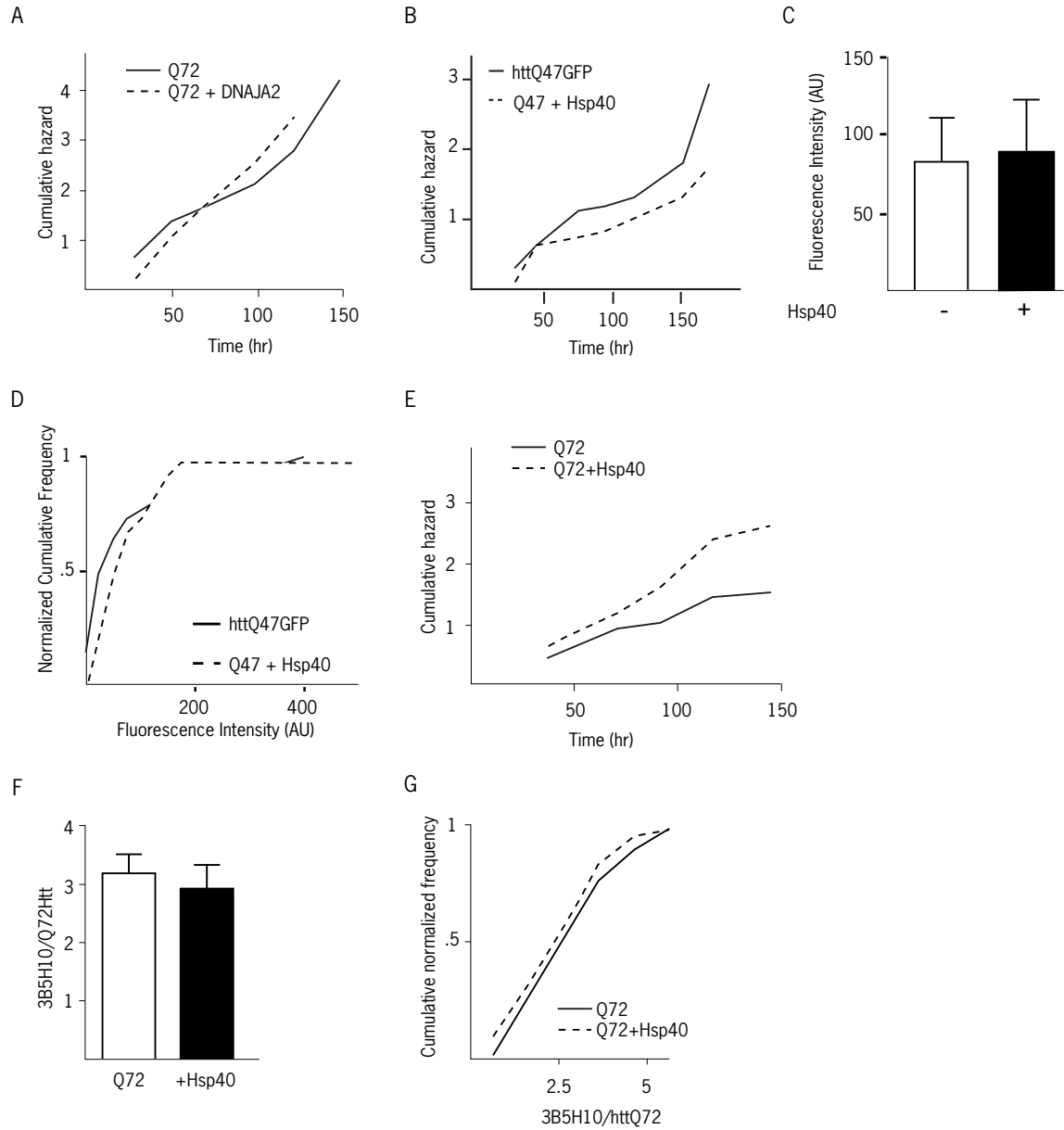


Figure A.2. Hsp40 or DNAJA2 have no consistent effect on survival in cells with mutant htt. E17-19 striatal cells were transfected 5-7 DIV with 1 μ g each of Hsp40 (plasmid library location: E35), pGW1-DNAJA2 (P. Muchowski) or pcDNA3.1(+) in addition to pGW1-httQ72GFP and pcDNA3.1(+)-mRFP. Some experiments showed no effect (A), a beneficial effect (B) or detrimental effect (C) on httQ72GFP toxicity. In the experiment with a slight beneficial effect, addition of Hsp40 had no effect on htt levels (D,E). In parallel experiments, Hsp40 had no effect on relative availability of the 3B5H10 epitope (F,G).

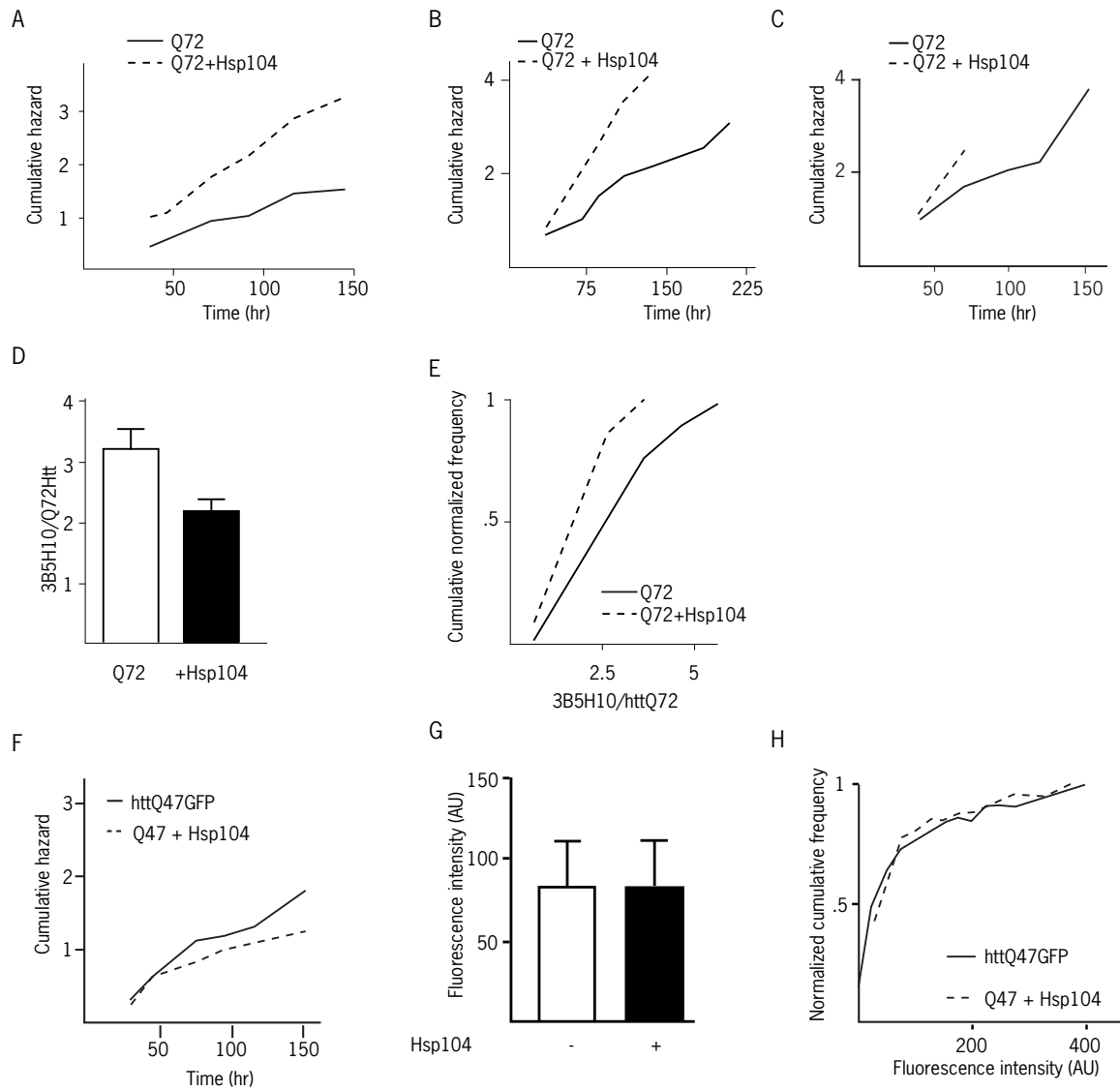


Figure A.3. Hsp104 generally increases the toxicity of mutant htt. E17-19 striatal cells were transfected 5-7 DIV with 1 μ g each of Hsp104 (plasmid library location: K51) or pcDNA3.1(+) in addition to pGW1-httQ72GFP and pcDNA3.1(+)-mRFP. Three experiments (A-C) demonstrated a significant toxic effect of Hsp104 with a parallel experiment showing a reduction in the relative amount of available 3B5H10 epitope (D,E). One experiment with pGW1-httQ47GFP demonstrated no effect on survival (F) or htt levels (G,H).

Ubiquitin-proteasome system

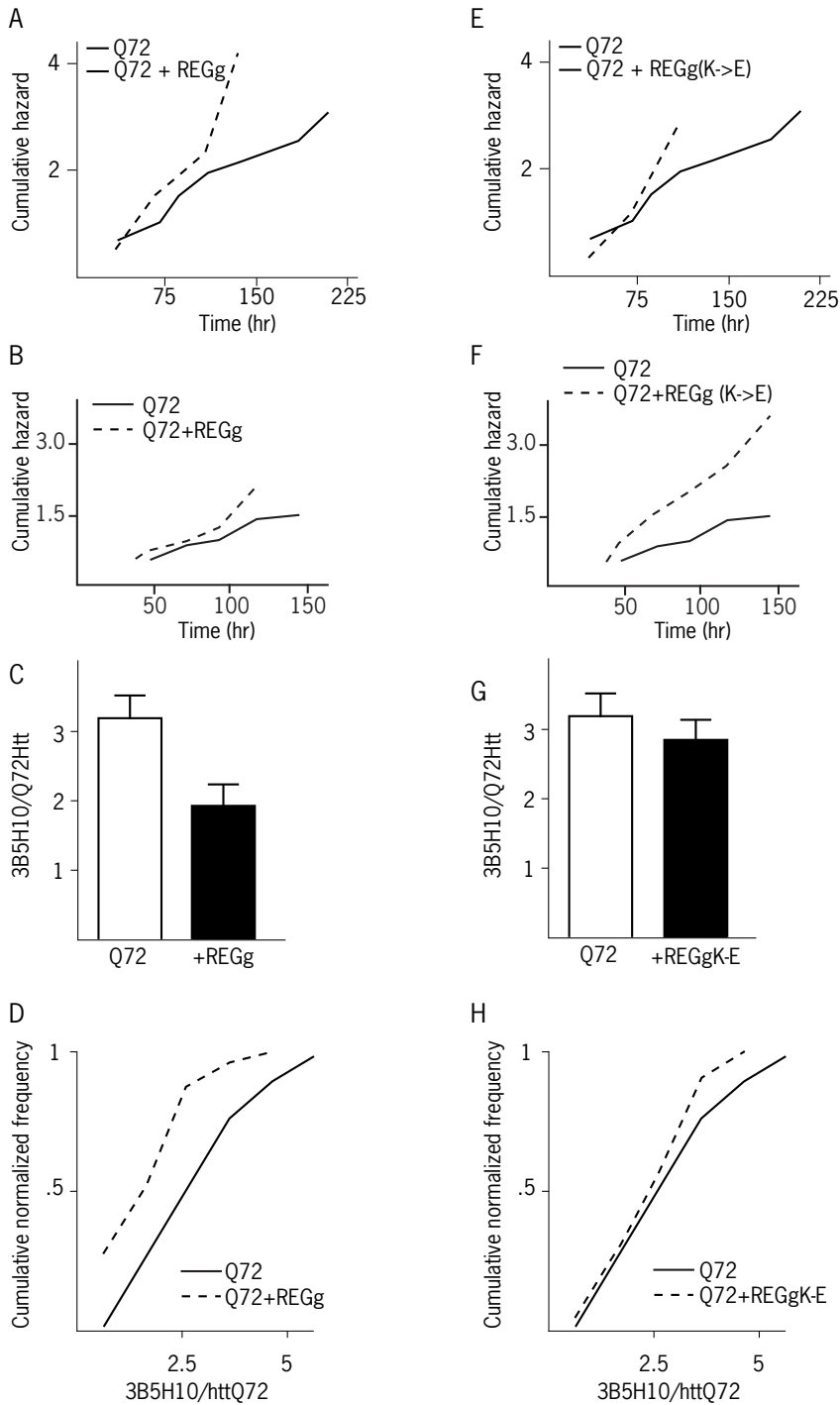


Figure A.4. REGg and REGg(K->E) increase the toxicity of mutant htt. E17-19 striatal cells were transfected 5-7 DIV with 1 μ g each of REGg (plasmid library location: Q53), REGg(K->E) (plasmid library location: Q55) or pcDNA3.1(+) in addition to pGW1-httQ72GFP and pcDNA3.1(+)-mRFP. Both REGgs potentiated the toxicity of mutant htt (A,B,E,F) but only REGg (wt) decreased the relative amount of available 3B5H10 epitope (C,D).

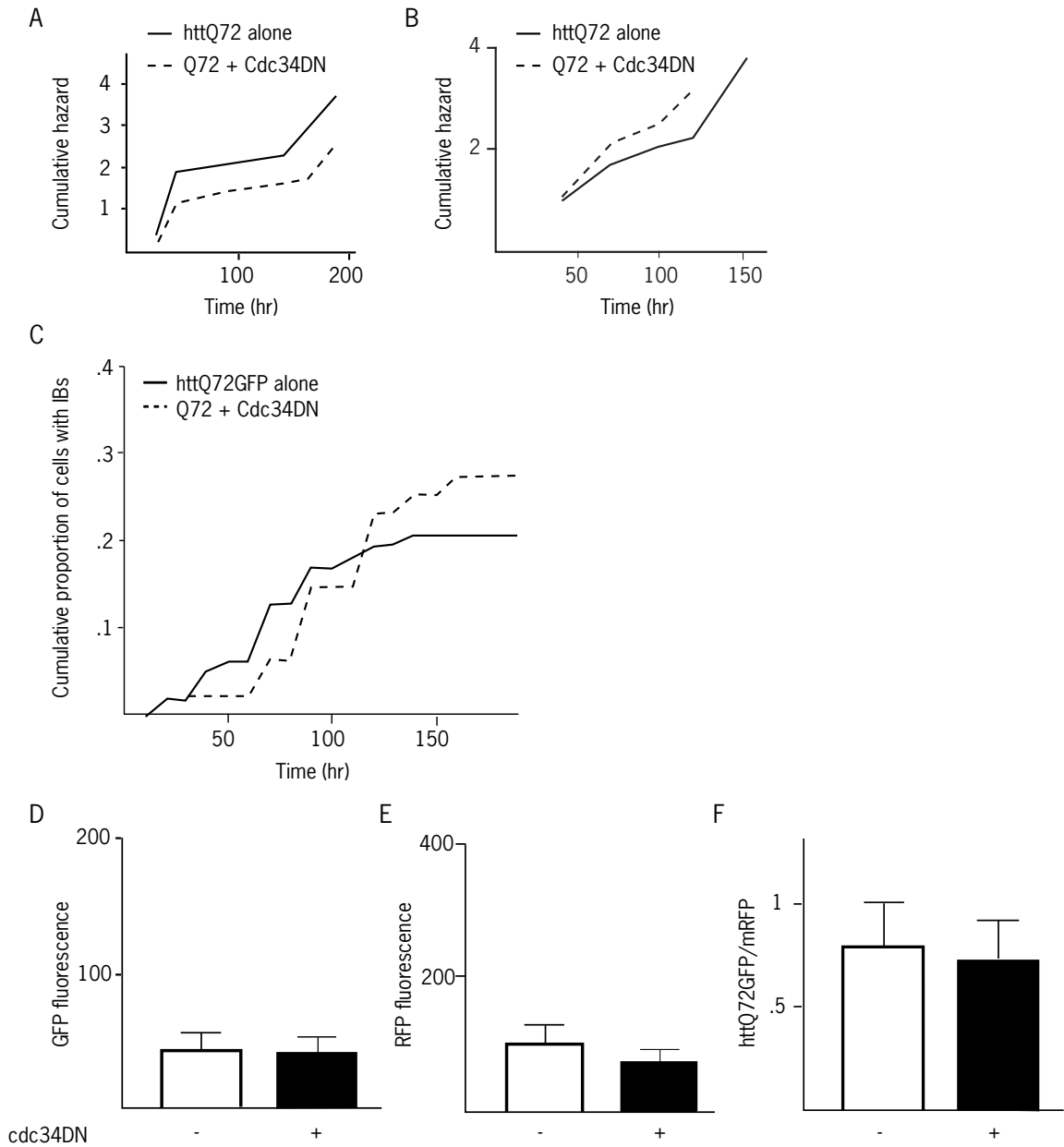


Figure A.5. *cdc34DN* has no consistent effect on mutant *htt* toxicity. E17-19 striatal cells were transfected 5-7 DIV with 1 μ g each of hCdc34(CL \rightarrow S) (plasmid library location: F20) or pcDNA3.1(+) in addition to pGW1-httQ72GFP and pcDNA3.1(+)-mRFP. Dominant negative *cdc34* protected against *htt* toxicity in some experiments (A) while potentiating toxicity in others (B). In experiments where there was a beneficial effect, there was no large effect on IB formation (C), *htt* or mRFP levels (D-F).

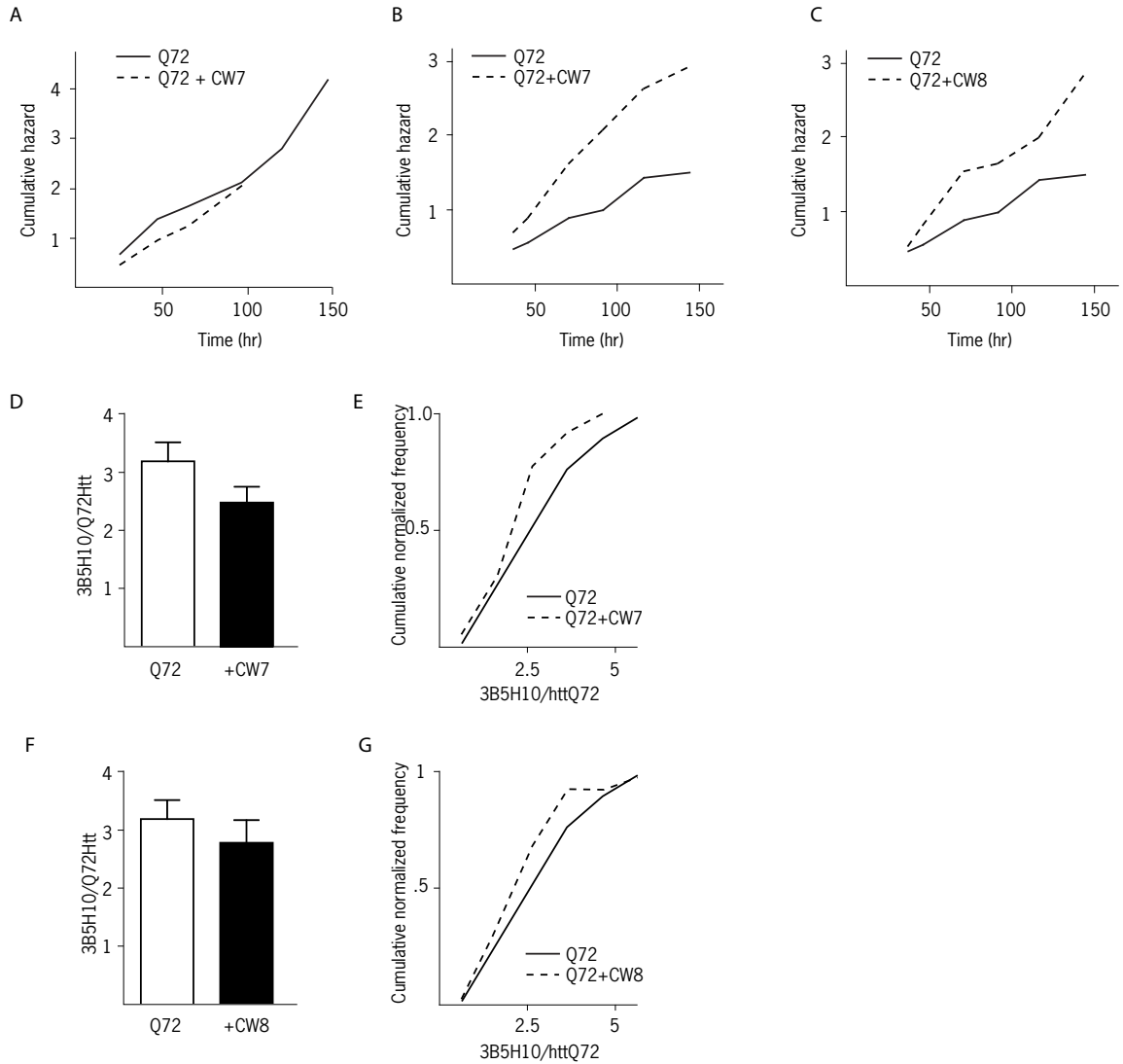


Figure A.6. Wild-type or chain terminating ubiquitin potentiate mutant htt toxicity. E17-19 striatal cells were transfected 5-7 DIV with 1 μ g each of wild-type ubiquitin (CW7; plasmid library location: F17), chain-terminating ubiquitin (CW8; plasmid library location: F16) or pcDNA3.1(+) in addition to pGW1-httQ72GFP and pcDNA3.1(+)-mRFP. CW7 had no effect in one experiment (A) while both CW7 and CW8 were toxic in a second (B,C). In a parallel experiment, CW7 (D,E) and to a lesser extent, CW8 (F,G), decreased the relative availability of the 3B5H10 epitope.

Autophagy

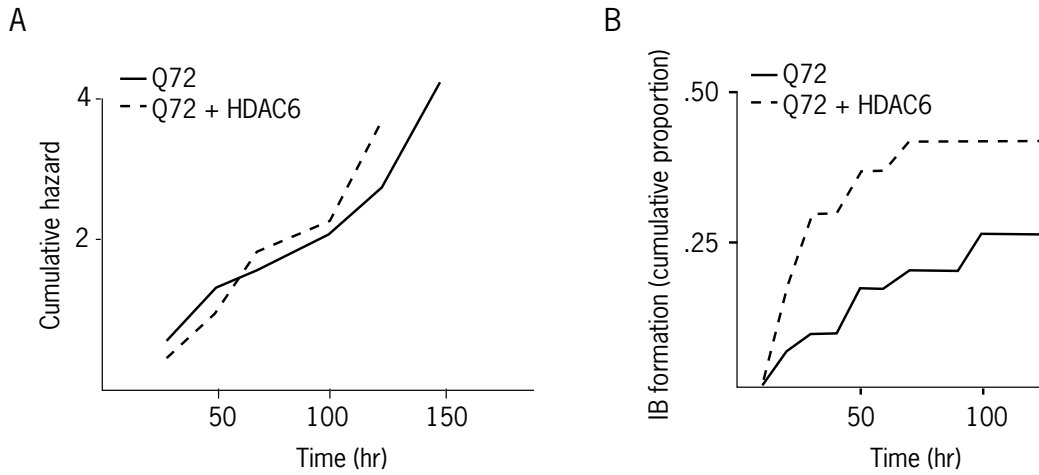


Figure A.7. HDAC6 has no effect on mutant htt toxicity but increases mutant htt IB formation. E18 striatal cells were transfected 7 DIV with 1 μ g each of HDAC6 (plasmid library location: O63) or pcDNA3.1(+) in addition to pGW1-httQ72GFP and pcDNA3.1(+)-mRFP. Addition had no effect on survival (A) but increased the rate of IB formation and proportion of cells forming IBs (B).

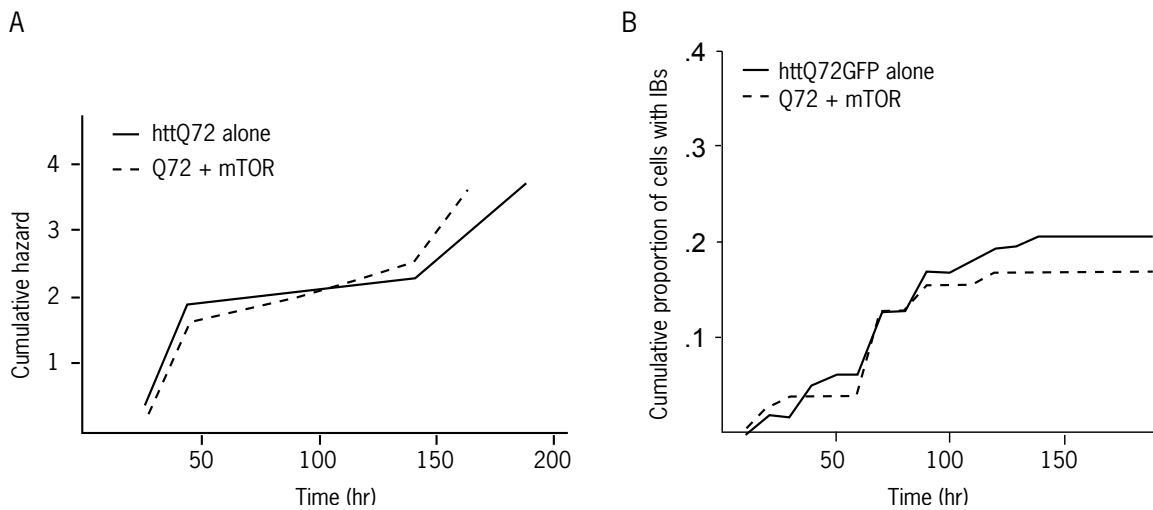


Figure A.8. mTOR has no effect on mutant htt toxicity or IB formation. E18 striatal cells were transfected 7 DIV with 1 μ g each of mTOR (plasmid library location: R43) or pcDNA3.1(+) in addition to pGW1-httQ72GFP and pcDNA3.1(+)-mRFP. mTOR overexpression had no effect on mutant htt toxicity (A) or IB formation (B).

Interacting proteins

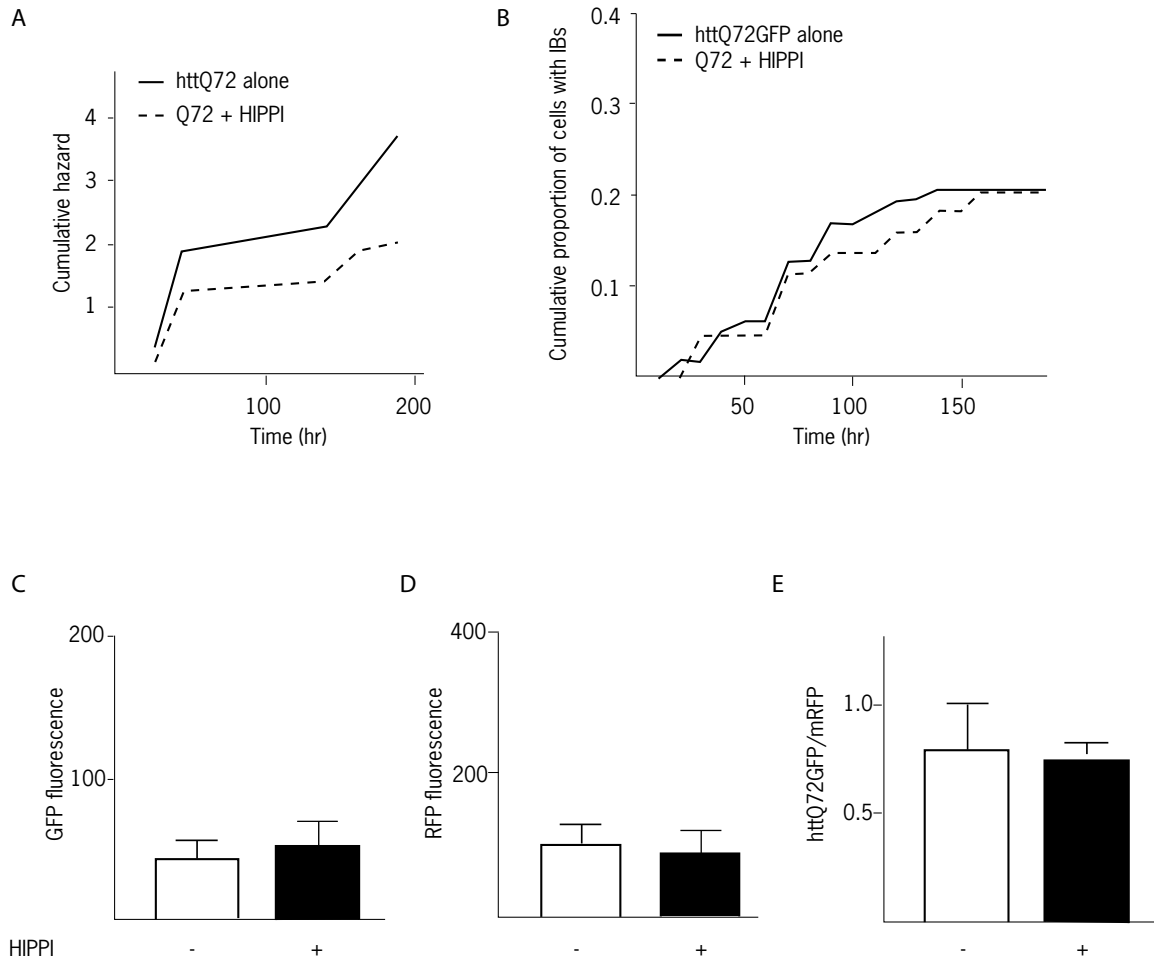


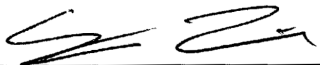
Figure A.9. HIPPI decreases mutant htt toxicity but has no effect on IB formation or htt levels. E18 striatal cells were transfected 7 DIV with 1 μ g each of HIPPI (plasmid library location: O69) or pcDNA3.1(+) in addition to pGW1-httQ72GFP and pcDNA3.1(+)-mRFP. HIPPI decreased httQ72 toxicity (A) but had no effect on IB formation (B) or protein levels (C-E).

Publishing Agreement

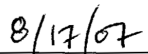
It is the policy of the University to encourage the distribution of all theses and dissertations. Copies of all UCSF theses and dissertations will be routed to the library via the Graduate Division. The library will make all theses and dissertations accessible to the public and will preserve these to the best of their abilities, in perpetuity.

Please sign the following statement:

I hereby grant permission to the Graduate Division of the University of California, San Francisco to release copies of my thesis or dissertation to the Campus Library to provide access and preservation, in whole or in part, in perpetuity.



Author Signature



Date